Mini-barcodes are equally useful for species identification and more suitable for large-scale species discovery in Metazoa than full-length barcodes

Running Title: mini-barcodes for species discovery

Darren Yeo[1], Amrita Srivathsan[1], Rudolf Meier[1*]

[1]Department of Biological Sciences, National University of Singapore, 14 Science 8 Drive 4, Singapore 117543

[*]Corresponding author: meier@nus.edu.sg

Abstract

New techniques for the species-level sorting of millions of specimens are needed in order to accelerate species discovery, determine how many species live on earth, and develop efficient biomonitoring techniques. These sorting methods should be reliable, scalable and cost-effective, as well as being largely insensitive to low-quality genomic DNA, given that this is usually all that can be obtained from museum specimens. Mini-barcodes seem to satisfy these criteria, but it is unclear how well they perform for species-level sorting when compared to full-length barcodes. This is here tested based on 20 empirical datasets covering ca. 30,000 specimens and 5,500 species, as well as six clade-specific datasets from GenBank covering ca. 98,000 specimens for over 20,000 species. All specimens in these datasets had full-length barcodes and had been sorted to species-level based on morphology. Mini-barcodes of different lengths and positions were obtained *in silico* from full-length barcodes using a sliding window approach (3 windows: 100-bp, 200-bp, 300-bp) and by excising nine mini-barcodes with established primers (length: 94 – 407-bp). We then tested whether barcode length and/or position reduces species-level congruence between morphospecies and molecular Operational Taxonomic Units (mOTUs) that were obtained using three different species delimitation techniques (PTP, ABGD, objective clustering). Surprisingly, we find no significant differences in performance for both species- or specimen-level identification between full-length and mini-barcodes as long as they are of moderate length (>200-bp). Only very short mini-barcodes (<200-bp) perform poorly, especially when they are located near the 5' end of the Folmer region. The mean congruence between morphospecies and mOTUs is ca. 75% for barcodes >200-bp and the congruent mOTUs contain ca. 75% of all specimens. Most conflict is caused by ca. 10% of the specimens that can be

identified and should be targeted for re-examination in order to efficiently resolve conflict. Our study suggests that large-scale species discovery, identification, and metabarcoding can utilize mini-barcodes without any demonstrable loss of information compared to full-length barcodes.

Keywords: DNA barcoding, mini-barcodes, species discovery, metabarcoding

Introduction

The question of how many species live on earth has intrigued biologists for centuries, but we are nowhere close to having a robust answer. We do know that fewer than 2 million have been described and that there are an estimated 10-100 million multicellular species on the planet (Roskov et al. 2018). We also know that many are currently being extirpated by the “sixth mass extinction” (Ceballos et al. 2015; Sánchez-Bayo and Wyckhuys 2019), with potentially catastrophic consequences for the environment (Cafaro 2015). Monitoring, halting, and perhaps even reversing this process is frustrated by the “taxonomic impediment”. This impediment is particularly severe for “invertebrates” that collectively contribute much of the animal biomass (e.g., Stork et al. 2015; Bar-On et al. 2018). Most biologists thus agree that there is a pressing need for accelerating species discovery and description. This very likely requires the development of new molecular sorting methods because the traditional approach involving parataxonomists or highly-trained taxonomic experts is either too imprecise (Krell 2004) or too slow and expensive. However, any replacement method based on DNA sequences should be accurate, but also (1) rapid, (2) cost-effective and (3) and largely insensitive to DNA quality. These criteria are important because tackling the earth’s biodiversity will likely require the processing of >500 million specimens, even under the very conservative assumption that there are only 10 million species (Stork 2018) and a new species is discovered with every 50 specimens processed. Cost-effectiveness is similarly important because millions of species are found in countries with limited funding and only basic research facilities. On the positive side, many species are already represented as unsorted material in museum holdings, but such specimens often yield degraded DNA (Cooper 1994). Therefore, methods that require DNA of

high-quality and quantity are not likely to be suitable for large-scale species discovery in invertebrates.

High-throughput species discovery with barcodes

Conceptually, species discovery and description can be broken up into three steps. The first is obtaining specimens, the second, species-level sorting, and the third, species identification or description. Fortunately, centuries of collecting have gathered many of the specimens that are needed for large-scale species discovery. Indeed, for many invertebrate groups it is likely that the museum collections contain more specimens of undescribed than described species; i.e., this unsorted collection material represents vast and still underutilized source for species discovery (Lister et al. 2011; Kemp 2015; Yeates et al. 2016). The second step in species discovery/description is species-level sorting, which is in dire need of acceleration. Traditionally, it starts with sorting unsorted material into major taxa (e.g., order-level in insects). This task can be accomplished by parataxonomists but may in the future be guided by robots utilizing neural networks (Valan et al. 2019). In contrast, the subsequent species-level sorting is usually time-limiting because the specimens for many invertebrate taxa have to be dissected and slide-mounted before they can be sorted to species-level by highly-skilled specialists; i.e., the traditional techniques are neither rapid nor cost-effective. This impediment is likely to be responsible for why certain taxa that are known to be abundant and species-rich are particularly poorly studied (Bickel 1999).

An alternative way to sort specimens to species-level would be with DNA sequences. This approach is particularly promising for metazoan species because most multicellular animal species can be distinguished based on cytochrome c

100 oxidase subunit I (*cox1*) barcode sequences (Hebert et al. 2003). However, such
101 sorting requires that every specimen is barcoded. This creates cost- and scalability
102 problems when the barcodes are obtained with Sanger sequencing (see Taylor and
103 Harris 2012). Such sequencing is currently still the standard in many barcoding
104 studies because the animal barcode was defined as a 658-bp long fragment of *cox1*
105 ("Folmer region": Folmer et al. 1994), although sequences >500-bp with <1%
106 ambiguous bases are also considered BOLD-compliant (Barcode Of Life Data
107 System: BOLDsystems.org). The 658-bp barcode was optimized for ABI capillary
108 sequencers but it has become a burden because it is not suitable for cost-effective
109 sequencing with Illumina platforms.

110 Due to these constraints, very few studies have utilized DNA barcodes to sort
111 entire samples into putative species (but see Fagan-Jeffries et al. 2018). Instead,
112 most studies use a mixed approach where species-level sorting is carried out based
113 on morphology before a select few specimens per morphospecies are barcoded (e.g.
114 Riedel et al. 2010). Unfortunately, this two-step process requires considerable
115 amounts of skilled manpower and time and does not allow for an unbiased
116 assessment of congruence-levels between morphology and DNA barcodes.

117 *Obtaining Barcodes with High Throughput Sequencing*

118 Fortunately, scalability and cost-effectiveness are hallmark features of the
119 new high throughput sequencing (HTS) technologies. These technologies are
120 particularly suitable for sequencing the kind of degraded DNA that is typical of
121 museum specimens. Indeed, hybrid capture has already been optimized for the use
122 with old museum specismens (Bi et al. 2013; Guschanski et al. 2013; Blaimer et al.
123 2016) and is likely to play a major role for the integration of rare species into

124 taxonomic and systematic projects. It will be difficult and expensive, however, to
125 apply enrichment methods to millions of specimens because such methods require
126 time-consuming and expensive molecular protocols (e.g., specimen-specific
127 libraries). Fortunately, for most species the initial species-level pre-sorting can be
128 achieved using barcodes that can be obtained via “tagged amplicon sequencing” on
129 a variety of next-generation sequencing platforms ("NGS barcodes”: Wang et al.
130 2018; Yeo et al. 2018).

131 Until recently, obtaining full-length NGS barcodes via tagged amplicon
132 sequencing was difficult because the reads of most next-generation-sequencing
133 platforms were too short for sequencing the full-length barcode. This has now
134 changed with the arrival of third-generation platforms (ONT: MinION: Srivathsan et
135 al. 2018, 2019; PacBio: Sequel: Hebert et al. 2018). These platforms, however,
136 come with drawbacks; *viz* elevated sequencing error rates and higher cost. These
137 problems are likely to be overcome in the future (e.g. Yang et al. 2018), but this
138 would still not solve the main challenge posed by full-length barcodes; i.e., problems
139 with reliably obtaining amplicons from museum specimens with degraded DNA (e.g.
140 Hajibabaei et al. 2006). We thus submit that it is time to use empirical evidence to
141 determine at which length and in which position mini-barcodes are as effective for
142 pre-sorting specimens into putative species as full-length barcodes.

143 *Mini-barcodes*

144 Barcodes that are shorter than the full-length barcode are often referred to as
145 “mini-barcodes”. They are obtained with primers that amplify shorter subsets of the
146 original barcode region and have three key advantages. Firstly, mini-barcodes are
147 predicted to amplify more readily when the DNA in the sample is degraded. This was

148 confirmed by several studies comparing amplification success rates for mini- and full-
149 length barcodes for the same DNA template (Hajibabaei et al. 2006; Meusnier et al.
150 2008; Hajibabaei and McKenna 2012). This property makes mini-barcodes the
151 preferred choice for barcoding museum specimens that had been stored under
152 suboptimal conditions for decades. The ease of amplification is also one of the
153 reasons why mini-barcodes are the default for metabarcoding projects that rely on
154 environmental DNA with widely varying DNA quality [e.g., gut content, faeces
155 (Deagle et al. 2006)].

156 A second benefit of mini-barcodes is that they can be sequenced at low cost
157 on short-read sequencing platforms (e.g., Illumina). The maximum amplicon lengths
158 that such platforms can accommodate is ~450-bp including primer length (using 250-
159 bp paired-end sequencing libraries), which necessitates the amplification and
160 sequencing of two overlapping regions to recover the entire 658-bp barcode
161 (Shokralla et al. 2015b). However, given the additional time and resources required,
162 it begs the question if there is much to be gained by investing in full-length barcodes.
163 Full-length barcodes are often automatically assumed to improve performance but
164 more data does not automatically yield better results. There is often a saturation
165 point beyond which additional data have little impact on results while increasing
166 consumable and manpower cost. Occasionally, more data can even be detrimental.
167 For example, fast-evolving genes or third positions in protein-encoding genes can
168 worsen the results of phylogenetic analyses addressing the relationships between
169 old clades. Note that this could also be a concern for barcodes, because sequence
170 variability changes across the Folmer region of COI (Roe and Sperling 2007;
171 Pentinsaari et al. 2016). Overall, it is important that one should use empirical data to
172 determine how long barcodes have to be in order to be informative.

173 Unfortunately, the performance of mini-barcodes remains insufficiently tested
174 despite their ubiquitous use in metabarcoding. The existing tests suffer from lack of
175 scale (the largest study includes 6695 barcodes for 1587 species: Meusnier et al.
176 2008) or taxonomic scope (usually only 1-2 family-level taxa: e.g. Hajibabaei et al.
177 2006; Yu and You 2010). Furthermore, the tests yielded conflicting results.
178 Hajibabaei et al. (2006) found high congruence with the full-length barcode when
179 species are delimited based on mini-barcodes and Meusnier et al. (2008) find similar
180 BLAST identification rates for mini-barcodes and full-length barcodes in their *in silico*
181 tests. However, Yu and You (2010) conceded that mini-barcodes may have worse
182 accuracy despite having close structural concordance with the full-length barcode. In
183 addition, Sultana et al. (2018) concluded that the ability to identify species is
184 compromised when the barcodes are too short (<150-bp), but it remained unclear at
185 which length/position mini-barcodes stop performing poorly. Furthermore, published
186 tests of mini-barcodes compare their performance to results obtained with full-length
187 barcodes. All conflict is then considered evidence for the failure of mini-barcodes,
188 even though the Folmer region varies in nucleotide variability (Roe and Sperling
189 2007) and conflict alone does not settle which result is correct. Lastly, the existing
190 tests of mini-barcodes do not include a sufficiently large number of different mini-
191 barcodes in order to be able to detect positional and length effects across the 658-bp
192 barcode region.

193 Here, we address the lack of scale in previous tests by including 20 empirical
194 studies covering 5500 species (ca. 30,000 barcodes) and Genbank data for 20,673
195 species (ca. 98,000 barcodes). We test a large number of different mini-barcodes by
196 applying a sliding window approach to generate mini-barcodes of different lengths
197 (100, 200, 300-bp window length, 60-bp intervals) and compare the results to the

198 performance of nine mini-barcodes with established primers (mini-barcode length: 94
199 – 407-bp). The taxonomic scope of our study is broad and includes a wide variety of
200 metazoans ranging from earthworms to butterflies and birds. Lastly, we do not
201 assume that mOTUs based on full-length barcodes are more accurate than those
202 obtained with mini-barcodes. Instead, we assess whether mOTUs obtained with
203 different-length barcodes have different levels of congruence with morphospecies;
204 i.e. morphology is treated as a constant and we only test whether barcode length
205 and/or position influence the number of morphospecies that are recovered. All
206 specimens that are mis-sorted based on morphology (e.g. due to the presence of
207 cryptic species) will be equally mis-sorted for the full-length barcodes and the mini-
208 barcodes that are derived from the former via shortening; i.e., misidentified
209 specimens become noise. What we assess is whether there is an additional loss of
210 congruence between barcodes and morphology as the barcode length shrinks or
211 mini-barcodes are in a different position within the Folmer region of COI.

212 We also compare the performance of different species delimitation methods.
213 There has been substantial interest in developing algorithms for mOTU estimation,
214 leading to the emergence of various species delimitation algorithms over the past
215 decade (e.g. objective clustering: Meier et al. 2006; BPP: Yang and Rannala 2010;
216 jmOTU: Jones et al. 2011; ABGD: Puillandre et al. 2012; BINs: Ratnasingham and
217 Hebert 2013; PTP: Zhang et al. 2013; etc.). For the purposes of this study, we
218 selected three algorithms that represent distance- and tree-based methods: objective
219 clustering, Automatic Barcode Gap Discovery (ABGD) and Poisson Tree Process
220 (PTP). Objective clustering utilizes an *a priori* distance threshold to group sequences
221 into clusters, ABGD groups sequences into clusters based on an initial prior and
222 recursively uses incremental priors to find stable partitions, while PTP utilizes the

223 branch lengths on the input phylogeny to delimit species units. Note that PTP is
224 frequently applied to trees derived from barcode data (e.g. Ermakov et al. 2015; Han
225 et al. 2016; Hollatz et al. 2016). There are numerous additional techniques for
226 species delimitation, but most require multiple markers and thus do not scale easily
227 to millions of specimens.

228 In addition to species delimitation, we also examine the utility of mini-
229 barcodes for species identification, which is the original use of DNA barcodes
230 (Hebert et al. 2003). Species identification with barcodes is particularly valuable for
231 the detection of specific species and community characterization via metabarcoding
232 studies (Ficetola et al. 2008; Lim et al. 2016; Morinière et al. 2019). Most of these
233 studies tend to involve poor quality genetic material (i.e., gut content, faecal matter,
234 environmental DNA) and hence it would be valuable to know whether short markers
235 can be reliably used to assign species names to unidentified mini-barcodes. We here
236 test the performance of the barcodes using "best close match", which considers
237 those sequences correctly identified when they match conspecific barcodes within a
238 predefined threshold (Meier et al. 2006).

239

240 **Materials & Methods**

241 *Dataset selection, alignment, excising in silico mini-barcodes*

242 We surveyed the barcoding literature in order to identify 20 recent publications
243 from 2007 – 2017 that cited the original barcode paper by Hebert et al. (2003) and
244 met the following criteria: 1) have specimens where the barcoded specimens were
245 pre-sorted/identified based on morphology and 2) the dataset had at least 500
246 specimens with *cox1* barcodes >656-bp (Table S1a). In addition, we compiled six

247 additional datasets based on sequences from GenBank for species-rich metazoan
248 taxa: Actinopterygii, Arachnida, Coleoptera, Diptera, Hymenoptera and Lepidoptera.
249 The clade names were used for taxonomy searches in NCBI and all mitochondrial
250 nucleotide sequences of length 657-1000 bp were downloaded. To these, we added
251 annotated *cox1* sequences from mitochondrial genomes (mitochondrial sequences
252 of length 10,000-20,000 bp). Subsequently, we filtered for the *cox1* gene using an
253 alignment to a reference full-length *cox1* barcode with MAFFT's --add function
254 (Katoh and Standley 2013), where any non-target sequences are easily identified by
255 large indels and discarded. We then removed all sequences that were shorter than
256 657-bp, introduced indels in the multiple sequence alignment, were not identified to
257 species, or included ambiguous species names. Four of the datasets (Actinopterygii:
258 21,390 barcodes, Coleoptera: 44,403 barcodes, Diptera: 56,344 barcodes,
259 Lepidoptera: 198,441 barcodes), were too large for a full evaluation using all species
260 delimitation methods. We therefore randomly selected 20,000 sequences (=RAND()
261 in Microsoft Excel) for further analysis. These six datasets comprised 97,758
262 barcodes for 20,673 morphospecies after subsampling (Table S1b).

263 The barcode sequences were downloaded from BOLDSystems or NCBI
264 GenBank and aligned with MAFFT v7 (Katoh and Standley 2013) with a gap opening
265 penalty of 5.0. Using a custom Python script, we generated three sets of mini-
266 barcodes along a "sliding window" for the 20 empirical datasets. They were of 100-,
267 200- and 300-bp lengths. The first iteration begins with the first base pair of the 658-
268 bp barcode and the shifting windows jump 60-bp at each iteration, generating ten
269 100-bp windows, eight 200-bp windows and six 300-bp windows. Additionally, we
270 identified nine mini-barcodes with published primers within the *cox1* Folmer region
271 (Fig. 1 & Table S2). These mini-barcodes have been repeatedly used in the literature

272 for a broad range of taxa. The primers for the various mini-barcodes were aligned to
273 the homologous regions of each dataset with MAFFT v7 --addfragments (Katoh and
274 Standley 2013) in order to identify the precise position of the mini-barcodes within
275 the full-length barcode. The mini-barcode subsets from each barcode were then
276 identified after alignment to full-length barcodes to mark the start and end-point of
277 the amplicon. Note that most of the published primers are in the 5' region of the full-
278 length barcode. The nine mini-barcodes with published primers were assessed for
279 the 20 empirical and for the six GenBank datasets.

280 *Species delimitation*

281 Mini-barcodes and full-length barcodes were clustered into putative species
282 using three species delimitation algorithms: objective clustering (Meier et al. 2006),
283 ABGD (Puillandre et al. 2012) and PTP (Zhang et al. 2013). For objective clustering,
284 the mOTUs were clustered at 2 – 4% uncorrected p-distance thresholds (Srivathsan
285 and Meier 2012) using a Python script which re-implements the objective clustering
286 of Meier et al. (2006) and allows for batch processing. The p-distance thresholds
287 selected are the typical distance thresholds used for species delimitation in the
288 literature (Meier et al. 2006, 2016; Ratnasingham and Hebert 2013). The same
289 datasets were also clustered with ABGD (Puillandre et al. 2012) using the default
290 range of priors and with uncorrected p-distances, but the minimum slope parameter
291 (-X) was reduced in a stepwise manner (1.5, 1.0, 0.5, 0.1) if the algorithm could not
292 find a partition. We then considered the ABGD clusters at priors P=0.001, P=0.01
293 and P=0.04. The priors (P) refer to the maximum intraspecific divergence and
294 function similarly to p-distance thresholds at the first iteration. In the ABGD
295 algorithm, they are refined by recursive application. Lastly, in order to use PTP, we
296 generated maximum likelihood (ML) trees in RAxML v.8 (Stamatakis 2014) via rapid

297 bootstrapping (-f a) under the GTRCAT model. For the 20 empirical datasets, the
298 best tree generated for each dataset was then used for species delimitation with PTP
299 (Zhang et al. 2013) under default parameters. For the six much larger clade-based
300 datasets, we used mPTP (Kapli et al. 2017) with the --single parameter as the
301 original algorithm took too long to yield results. In order to reduce computational time
302 for RAxML and PTP, haplotype representatives were used for the six Genbank
303 dataset instead of the entire dataset. The remaining barcodes with identical
304 haplotypes were then mapped back into the same mOTU clusters using their
305 respective haplotypes.

306 *Performance assessment*

307 The performance of mini-barcodes was assessed using morphospecies as an
308 external arbiter. Species-level congruence was quantified using match ratios
309 between molecular and morphological groups (Ahrens et al. 2016). The ratio is
310 defined as $\frac{2 \times N_{match}}{N_1 + N_2} \times 100$, where N_{match} is the number of clusters identical across
311 both mOTU delimitation methods/thresholds (N_1 & N_2). Consolidated match ratios
312 are derived by first summing relevant all numerator and denominator values before
313 calculating the ratio. Incongruence between morphospecies and mOTUs is usually
314 caused by a few specimens that are assigned to the “incorrect” mOTUs. Conflict at
315 the specimen-level can thus be quantified as the number of specimens that are in
316 mOTUs that cause conflict with morphospecies.

317 In order to test whether barcode length is a significant predictor of
318 congruence, MANOVA tests were carried out in R (R Core Team 2017) with “match
319 ratio” (species-level congruence) as the response variable and “dataset” and “mini-
320 barcode” as categorical explanatory variables. We found that most of the variance in

321 our study was generated by the variable “dataset” ($P < 0.05$ in MANOVA tests).
322 Given that we were interested in the effect of barcode length and position, “dataset”
323 was subsequently treated as a random effect and “mini-barcode” as the explanatory
324 variable (categorical) in a linear mixed effects model (R package *lme4*: Bates et al.
325 2014). The *emmeans* R package (Lenth 2018) was then used to perform pairwise
326 post-hoc Tukey tests between mini- and full-length barcodes so as to assess
327 whether either barcode was performing significantly better/worse. To compare the
328 differences in performance between objective clustering, ABGD and PTP, ANOVA
329 tests were performed in R. After which, pairwise Tukey tests were used to determine
330 which species delimitation method was responsible for significant differences. Lastly,
331 in order to explore the reasons for positional effects, the proportion of conserved
332 sites for each mini-barcode was obtained using MEGA6 (Tamura et al. 2013).

333 Match ratios indicate congruence at the species level, but it is also important
334 to determine how many specimens have been placed into congruent units. Note that
335 species- and specimen-level congruence are only identical when all mOTUs are
336 represented by the same number of specimens. However, specimen abundances
337 are rarely equal across species and hence match ratio is insufficient at
338 characterizing congruence between mOTUs and morphospecies. It is straightforward
339 to determine the number of congruent specimens as follows:

340 (1) Congruence Class I specimens: If $\boldsymbol{A} = \boldsymbol{B}$ then number of congruent specimens is
341 $Nc_1 = |A| \text{ OR } |B|$.

342 Lack of congruence is caused by morphospecies that are split, lumped, or
343 both split and lumped in the mOTUs. This means that a single mis-sorted specimen
344 placed into a single, large-sized mOTU leads to all specimens in two mOTUs to be

345 considered “incongruent” according to the criterion outlined above. Yet, most
346 specimens are congruent and full congruence could be restored by re-assigning the
347 mis-sorted specimen after re-examination. It is therefore also desirable to determine
348 the number of specimens that require re-examination or, conversely, the number of
349 specimens that would be congruent if one were to remove a few incongruent
350 specimens. This number of specimens can be estimated by counting congruent
351 specimens as follows:

352 (2) Congruence Class II specimens: Specimens that are in split or lumped mOTUs
353 relative to morphospecies. Here, the largest subset of congruently placed specimens
354 can be determined as follows. If $\boldsymbol{A_1} \cup \boldsymbol{A_2} \cup \ldots \cup \boldsymbol{A_x} = \boldsymbol{B}$: $Nc_2 = \max(|A_1|, |A_2| \ldots |A_x|)$

355 (3) Congruence Class III specimens: This covers specimens in sets of clusters that
356 are both split and lumped relative to morphospecies. Here, only those specimens are
357 considered potentially congruent that (1) are in one mOTU and one morphospecies
358 and (2) combined exceed the number of the other specimens in the set of clusters. In
359 detail, if $\boldsymbol{A_1} \cup \boldsymbol{A_2} \cup \ldots \cup \boldsymbol{A_x} = \boldsymbol{B_1} \cup \boldsymbol{B_2} \cup \ldots \cup \boldsymbol{B_y}$: $Nc_3 = \max(|A_1 \cap B_1|, |A_2 \cap$
360 $B_1| \ldots |A_x \cap B_y|)$ only if $\max(|A_1 \cap B_1|, |A_2 \cap B_1| \ldots |A_x \cap B_y|) > \frac{1}{2}(|A_1 \cup A_2 \ldots A_x|)$.

361 Note that these are approximate (over)estimates because we did not re-cluster
362 specimens after the removal of the specimens that were causing incongruence in the
363 original sets of clusters.

364 *Species identification*

365 Using the full-length and mini-barcode sets corresponding to published
366 primers, we assessed whether the barcodes were yielding conspecific matches
367 according to “best close match” implemented in SpeciesIdentifier program
368 (TaxonDNA: Meier et al. 2006). “Best close match” examines one barcode at a time.

369 It considers it unidentified and then determines whether the best-matching reference
370 sequence in the dataset is conspecific and within a user-defined distance threshold.
371 The distance threshold used for all assessments was 2%, which corresponds to the
372 best match ratio performance results for objective clustering in this study. Sequences
373 with conspecific matches within 2% are considered correctly identified, while
374 sequences that match allospecific sequences within 2% are considered incorrectly
375 identified. Sequences without matches within 2% are considered unidentified and
376 sequences that have both con- and allo-specific matches within the threshold are
377 considered to have an ambiguous identification. Mixed effects models were again
378 used to assess the performance of barcodes of different length. Similarly, pairwise
379 Tukey tests were used to test for statistical significance with the proportion of correct
380 matches as the response variable in order to determine whether the full-length
381 barcode performed significantly better than the mini-barcodes.

382 *Amplification success rates for 313-bp and 658-bp amplicons*

383 We tested amplification success rates for 47-48 specimens (~1mm) from six
384 Malaise trap samples of different age (2012 and 2018). The same genomic DNA was
385 used for each specimen for the amplification of the full-length barcode and a mini-
386 barcode of 313-bp length in two separate PCRs using different tagged primers:
387 HCO2198 (5'-TAAACTTCAGGGTGACCAAAAAATCA-3') and LCO1490 (5'-
388 GGTCAACAAATCATAAAGATATTGG-3') (658-bp; Folmer et al. 1994), mlCOIintF
389 (5'-GGWACWGGWTGAACWGTWTAYCCYCC-3') and jgHCO2198 (5'-
390 TAIACYTCIGGRTGICCRAARAAYCA-3') (313-bp; Leray et al. 2013). The PCR
391 reagents used were 5.0µl Taq MasterMix (CW0682; CWBio, Beijing, China), 1.0µl
392 RNase-free water, 0.5µl bovine serum albumin (1.0 mM), 0.5µl $MgCl_2$, 1.0µl of each
393 primer and 1.0µl of genomic DNA extract. The PCRs were run at 95°C for 5min, with

394 35 cycles of 94°C for 1min, 45°C for 2min and 72°C for 1min, and a final extension at
395 72°C for 5min. PCR amplification success was assessed using a 1% agarose gel,
396 with the electrophoresis run at 90V for 30min. Band presence was tabulated and chi-
397 squared performance testing was performed in R (R Core Team 2017).

398

399 **Results**

400 *Evaluation of mini-barcode congruence with morphology*

401 For species delimitation with objective clustering, we found that the 2% p-
402 distance threshold yielded the highest congruence-levels across the datasets. It was
403 hence used as the upper-bound estimator for assessing species- and specimen-level
404 congruence (see supplementary materials for corresponding results for the 3 and 4%
405 p-distances). For ABGD, average congruence was maximized for the prior P=0.001
406 and this prior was used in the main analysis (see supplementary material for results
407 under P=0.01 and P=0.04). PTP does not require *a priori* parameter choices. Overall
408 consolidated match ratio values range from 68 – 74% for these selected parameters
409 (Fig. 3), with the 20 empirical datasets generally performing better than the six clade-
410 based datasets (empirical/clade-based: OC at 2%: 81/72%; ABGD P=0.001: 76/69%;
411 PTP: 76/66%). Overall match ratios for the other objective clustering and ABGD
412 parameters tested range from 61 – 74% (Fig. S6).

413 The MANOVA tests performed on all treatments (species delimitation method
414 and distance threshold/prior) indicated that the test variable “dataset” was
415 responsible for much of the observed variance in our measure of congruence
416 (“match ratio”). The choice of mini-barcode or algorithm for generating mOTUs was
417 of secondary importance (Table S3). After accounting for “dataset”, we find that only

418 mini-barcodes <200-bp perform significantly worse than full-length barcodes (Fig. 2).
419 This is evident from the large number of significant differences ($p < 0.05$ & $p < 0.001$)
420 in pairwise post-hoc Tukey tests applied to 100-bp mini- and 657-bp full-length
421 barcodes. Only short barcodes (<100-bp) have a mean performance that is worse
422 (<0 match ratio deviation) than the full-length barcode. Conversely, for mini-
423 barcodes >200-bp, congruence with morphospecies does not differ significantly and
424 is occasionally superior to what is observed for the full-length barcode. Across all
425 datasets (20 empirical and 6 clade-based), species delimitation methods, and
426 clustering parameters (Fig. 3 & S6), the full-length barcode have the highest
427 congruence values in 49 of the 182 tests, but in 8 of these cases it is a tie and in an
428 additional 19 some mini-barcodes are within 0.5%. Furthermore, there is no
429 significant difference between the 200-bp and 300-bp mini-barcodes and the full-
430 length barcode when objective clustering or PTP are used to estimate mOTUs.
431 However, for all mOTU delimitation methods, the variance across datasets declines
432 as the mini-barcode increases in length (Fig. 2). The results obtained for *in silico*
433 mini-barcodes are broadly consistent with the performance of mini-barcodes
434 corresponding to published primers: the mini-barcodes of 94-bp, 130-bp, and 145-bp
435 lengths tend to perform worse than the longer mini-barcodes (Fig. 3). Congruence at
436 the species level is similar to congruence at the specimen level (Tables 1 & S8) with
437 some exceptions such as the performance improvements of short mini-barcodes, for
438 example, for the "French Guiana earthworms" when grouped with objective
439 clustering.

440 The results obtained for the 20 empirical datasets are similar to what is found
441 for the taxon-specific datasets consisting of sequences from GenBank. There are
442 small differences in match ratios for barcodes >200-bp and only very short barcodes

443 perform poorly. In many cases, the full-length barcode does not yield the best
444 performance compared to the mini-barcodes. An exception is the Coleoptera where
445 ABGD behaves erratically (Fig. 3). Short barcodes outperform long barcodes under
446 the lowest prior (P=0.001), but this trend reverses for higher priors.

447 With regard to specimen-based congruence, we focused on the mini-
448 barcodes with published primers that are >200-bp. For the 20 empirical datasets,
449 approximately three quarters of all specimens are in the "Congruence Class I"
450 (Tables 1 & S8); i.e., their placement is congruent between mOTUs and
451 morphospecies (Average/Median: OC at 2%: 77/77%; ABGD P=0.001: 74/74%;
452 PTP: 77/77%). The remaining specimens are placed in mOTUs that are split,
453 lumped, or split and lumped. The number of specimens that are responsible for
454 splitting and lumping are classified as Congruence Class II and III specimens (see
455 Materials and Methods). Overall, fewer than 10% of the specimens fall into these
456 categories (Table 1: see Class II specimens across species delimitation methods);
457 i.e., a fairly small number of specimens have to be studied when addressing conflict
458 between morphospecies and mOTUs. For the six clade-based datasets, there is
459 generally lower specimen congruence (Class I Average/Median: OC at 2%: 57/57%;
460 ABGD P=0.001: 53/54%; PTP: 57/57%), although this improves to ca. 75% at Class
461 II and ca. 80% at Class III. Note that a single mis-identified *D. melanogaster* could
462 result in all correctly identified specimens of this species to be considered
463 "incongruent" because they are no longer member of a congruent mOTU.

464 *Species delimitation method*

465 When the performance of the three different clustering methods was
466 compared, significant differences ($p < 0.05$ in ANOVA test) were found only for 100-

467 bp mini-barcodes (Fig. 4). Here, pairwise post-hoc Tukey tests find that objective
468 clustering performs significantly better than the other delimitation methods ($p <$
469 0.001) while ABGD and PTP do not differ significantly ($p = 0.88$) but behave
470 erratically for short mini-barcodes (Fig. 2).

471 *Positional effects*

472 Mini-barcodes situated at the 5' end of the full-length barcode perform
473 somewhat worse than those situated at the middle or at the 3' end (Fig. 2). For
474 example, the 100-bp mini-barcodes at the 5' end perform poorly for objective
475 clustering (mini-barcode midpoints at 50, 110 & 170-bp), ABGD (mini-barcode
476 midpoints at 110 & 170-bp) and PTP (mini-barcode midpoint at 110-bp). This effect
477 is, however, only statistically significant when the mini-barcodes are very short (100-
478 bp). This positional effect is observed across all species delimitation techniques.
479 Note that the 5' end of the full-length barcode appears to contain a large proportion
480 of conserved sites, particularly around the 170-bp and 230-bp midpoint of the 100-bp
481 mini-barcode (Fig. 5).

482 *Species identification performance*

483 When comparing the suitability of full-length and mini-barcodes for
484 identification purposes, we find that full-length barcodes frequently have the highest
485 number of correct matches (Table 2), but the differences are only statistically
486 significant for short mini-barcodes <200-bp: 94-bp: $p = <0.0001$, 130-bp: $p =$
487 <0.0001, 145-bp: $p = <0.0001$, 164-bp: $p = 0.0243$. All the remaining mini-barcodes:
488 (189 – 407-bp) have non-significant differences. Note that this is not due to scale
489 because we are using fairly large datasets here ($p = 0.0691 – 0.9996$). However, for
490 many datasets (e.g., Northwest Pacific Molluscs, North American Birds, etc.), the

491 proportion of ambiguous matches is higher for very short mini-barcodes (94-bp –
492 164-bp).

493 *Amplification success rates*

494 The 313-bp mini-barcode amplified significantly better than the full-length
495 barcode (472/570: 82.8% vs. 361/570: 63.3%; chi-squared test: p = <0.001) (Fig.
496 S9). Overall, the performance differences were greater for samples with overall low
497 amplification success rates (but see sample 4822).

498

499 **Discussion**

500 Accelerating species discovery and description are arguably foremost
501 challenges for the systematics of the 21st century because biodiversity is in steep
502 decline while systematists are still grappling with establishing the size and
503 distribution of the biodiversity that needs protection. Specimens for many
504 undescribed species are already in the world's natural history museums, but the
505 samples need to be sorted to species-level before they become available for species
506 identification/description and can be used for large-scale analyses of biodiversity
507 patterns. Pre-sorting specimens with DNA barcodes is a potentially promising
508 solution because it is scalable, can be applied to millions of specimens, and much of
509 the specimen handling can be automated. However, in order for this approach to be
510 viable, a sufficiently large proportion of the pre-sorted units need to accurately reflect
511 species boundaries. Furthermore, the methods should be suitable for processing
512 specimens that only yield degraded DNA. Mini-barcodes appear attractive on
513 technical grounds because sequencing short amplicons is cheap (Wang et al. 2018:
514 sequencing cost < 4 cents) and such amplicons have higher PCR amplification rates

515 especially if the DNA template is degraded. The latter has been repeatedly
516 discussed in the literature (Hajibabaei et al. 2006; Meusnier et al. 2008; Hajibabaei
517 and McKenna 2012) and was also confirmed here by comparing identification
518 success rates for a mini-barcode (313bp) and the full-full length barcode using the
519 same template (Fig. S9).

520 However, the use of mini-barcodes for species-level pre-sorting would
521 nevertheless have to be discouraged if full-length barcodes were to significantly
522 outperform mini-barcodes with regard to the accuracy of sorting specimens into
523 species. This is what we tested here and we find that mini-barcodes of moderate
524 length (>200 bp) perform as well as full-length barcodes.

525

526 *The main source of variance of congruence: datasets*

527 Overall, we here find that the average congruence between mOTUs and
528 morphospecies is 80% for all barcodes >200-bp (median: 83%) in the 20 empirical
529 datasets, with the median being higher (83%) because of a few outlier datasets with
530 low congruence <65% (OC at 2%; ABGD P=0.001, PTP). Similar variance is also
531 observed for the six clade-specific GenBank datasets. Both types of datasets were
532 tested because GenBank data are less likely to be affected by the idiosyncrasies of
533 individual study designs, but is known to contain misidentified sequences
534 (Mioduchowska et al. 2018). We overall find that the results are nevertheless similar
535 (Fig. 3 & S6) although the average congruence between mOTUs and morphospecies
536 is somewhat lower for GenBank datasets (mean=72%, median=71% for all
537 barcodes >200-bp across all three species delimitation methods and parameters).
538 Full-length barcodes only have the highest congruence level in 13 of the 42

539 treatments, but in 10 of those, the second highest congruence level for a mini-
540 barcode was only <0.5% lower. Mini-barcodes <200-bp perform poorly with the
541 possible exception of those for Coleoptera where mini-barcodes <200-bp perform
542 well under ABGD under two priors (Figs. 3 & S6: P=0.001, P=0.01).

543 Most studies assessing congruence levels between barcodes and morphology
544 focus on species-level congruence. However, specimen-level congruence is equally
545 important because the basic units in a museum collection or ecological surveys are
546 specimens. The correct placement of specimens into species is thus important for
547 systematists and biodiversity researchers alike given that the former would like to
548 see most of the specimens in a collection correctly placed and the latter often need
549 abundance and biomass information with species-level resolution. We find that for
550 the 20 empirical datasets, 74-77% (median) of the ca. 30,000 specimens are
551 assigned to species that are supported by molecular and morphological data even
552 under the strictest conditions (Table 1). Overall, this is a very high proportion
553 compared to species-level congruence obtained with species-level sorting by
554 parataxonomists (Krell 2004).

555 The remaining ca. 25% of specimens are placed in mOTUs whose boundaries
556 do not agree with morphospecies. One may initially consider this an unacceptably
557 high proportion, but it is important to keep in mind that the misplacement of one
558 specimen (e.g., due to a misidentification or contamination of a PCR product) will
559 render two mOTUs incongruent; i.e., all specimens in these mOTUs will be
560 considered incongruent and contribute to the 25% of “incongruently” placed
561 specimens. Arguably, one may instead want to investigate how many specimens are
562 causing the conflict. These are the specimens that should be targeted for re-
563 investigation in reconciliation studies using additional data. The proportion across the

564 20 datasets in our study is fairly low and ranges from 9-11% (median) depending on
565 which mOTU delimitation technique is used.

566 The six GenBank datasets however, have notably lower congruence-levels for
567 specimens (Class I median: 54-57%), with the Actinopterygii (47-48% median) and
568 Hymenoptera (45-47% median) having the poorest performance (Table S8). The
569 overall lower congruence could be caused by the misidentification of a few
570 specimens belonging to large mOTUs. This is supported by the greater difference
571 between Class I and Class III for the clade-based datasets as compared to the
572 empirical ones. Identifications from the empirical datasets are also more likely to be
573 standardized within the study and consequently have fewer potential conflicts
574 caused by differing taxon concepts associated with the same name (Franz 2005;
575 Meier 2017).

576 Conflict between mOTUs and morphospecies can be caused by technical
577 error or biology. A typical technical factor would be accidental misplacement of
578 specimens due to lab contamination or error during morphospecies sorting. Indeed,
579 the literature is replete with cases where mOTUs that were initially in conflict with
580 morphospecies became congruent once the study of additional morphological
581 characters let to the revision of morphospecies boundaries (e.g. Smith et al. 2008;
582 Tan et al. 2010; Baldwin et al. 2011; Ang et al. 2017). But there are also numerous
583 biological reasons why one should not expect perfect congruence between mOTUs
584 and species. Lineage sorting, fast speciation, large amounts of intraspecific
585 variability, and introgression are known to negatively affect the accuracy of DNA
586 barcodes (Will and Rubinoff 2004; Rubinoff et al. 2006; Meier 2008). It is thus
587 somewhat heartening that regardless of these issues, the final levels of congruence
588 between morphospecies and DNA sequences are often quite high in animals (Ball et

589 al. 2005; Cywinska et al. 2006; Renaud et al. 2012; Landi et al. 2014; Wang et al.
590 2018). This implies that pre-sorting specimens to species-level units based on
591 barcodes is worth pursuing for many metazoan clades. This realization led to the
592 proposal of the "reverse workflow" in Wang et al. (2018) who tested pre-sorting
593 based on sequences for 4,000 ant specimens. They found that 86 of the 89
594 molecular operational taxonomic units (mOTUs) were congruent with morphospecies
595 after reconciliation.

596 High levels of congruence levels are, however, not a universal observation
597 across all of life. There are groups with widespread barcode sharing between
598 species. Within Metazoa this is known for taxa such as Anthozoa (Huang et al. 2008)
599 and is likely to be the default outside of Metazoa (e.g. Chase and Fay 2009;
600 Hollingsworth et al. 2011). Indeed, congruence levels between mOTUs and
601 morphospecies also vary widely in the 20 empirical and 6 Genbank datasets studied
602 here (Fig. 3). Eighteen of the 26 datasets have congruence levels >75% and are
603 arguably doing well. With regard to the remaining eight, there are four where the low
604 levels may be due to the fact that they cover taxa or faunas that are comparatively
605 poorly known and sorting with morphology may be prone to error (French Guiana
606 Earthworms, Ecuadorian Chrysomelidae, chironomid midges in the genus
607 *Tanytarsus*). For a 5th data set, "Congolese fishes", the authors also mention
608 identification problems due to the lack of identification tools (Decru et al. 2016).
609 However, these problems should be lacking for Iberian butterflies where the authors
610 consider it likely that introgression and cryptic species are responsible for the lack of
611 congruence (Dincă et al. (2015). Note, however, that these problems do not appear
612 to affect the remaining Lepidoptera data set for which we observe high levels of
613 congruence (5 data sets). The picture is similarly confusing for fish (Actinopterygii)

614 where low congruence is observed for the Genbank dataset while marine fishes are
615 doing well (3 datasets). Similarly, inconsistent patterns are observed for
616 Hymenoptera and Arachnida.

617 We suspect that these inconsistent results are largely due to the lack of
618 rigorous studies that establish congruence with confidence. Such studies should be
619 based on datasets with dense taxon and geographic sampling where both
620 morphological and DNA sequence information is obtained for all specimens.
621 Subsequently, all specimens that cause conflict should be re-examined in order to
622 determine the proportion of specimens that were initially misplaced based on
623 morphology and the proportion that were initially misplaced based on DNA barcodes
624 (=pre-sorting error). Lastly, one should establish the number of specimens that
625 cannot be resolved because there is genuine conflict between the data sources.
626 Such studies are lacking. This also affects the quality of the morphospecies sorting
627 in the 26 datasets that are analzyed in our study. However, it should not affect our
628 overall conclusions with regard to the effect of barcode length and position on
629 congruence levels because morphospecies sorting errors affect both full-length
630 barcodes and the mini-barcodes that were excised from the former.

631 But what is gained if all specimens are sorted based on morphology and
632 barcodes? Using both sources of data would allow for higher quality work based on
633 the principles of integrative taxonomy (Dayrat 2005; Schlick-Steiner et al. 2010), but
634 it would not accelerate species discovery. Acceleration can only be achieved if either
635 a subset of all specimens have to be studied with morphology or the morphological
636 work requires less time. Both is the case when pre-sorting with barcodes is adopted.
637 This is shown in Wang et al. (2018) and Srivathsan et al. (2019), who pre-sorted
638 4000 ant and 7000 phorid specimens, respectively, with barcodes. Checking for

639 congruence between mOTUs and morpho-species was fast because the specimens
640 had already been pre-grouped into putative species based on barcodes. In addition,
641 determining the species limits between putatively closely related species was
642 simplified because the taxon-specialist could identify closely related
643 species/populations based on barcode distances. Lastly, for abundant species, only
644 a subset of the specimens had to be studied with morphology. This subset could be
645 selected based on genetic, temporal, and geographic gradients (Wang et al. 2018;
646 Srivathsan et al. 2019); i.e., the highly-skilled specialists could target a small
647 proportion of specimens for dissection and slide-mounting.

648 *Barcode length and species delimitation methods*

649 We here tested the widespread assumption that mOTUs based on full-length
650 barcodes are more reliable than those based on mini-barcodes (Burns et al. 2007;
651 Min and Hickey 2007). If this assumption was confirmed, then the use of mini-
652 barcodes for pre-sorting would have to be discouraged despite higher amplification
653 success rates and lower cost. However, we find that the performance of *cox1* mini-
654 barcodes with a length >200-bp do not differ substantially from the performance of
655 full-length barcodes. In 19/140 of the empirical and 3/42 of the clade-based dataset
656 treatments, the full-length barcode outperform all mini-barcodes, after discounting
657 ties (8/140 and 0/42) and cases where the difference between the next highest
658 congruence is <0.5% (9/140 and 10/42). Indeed, compared to the dataset effect, the
659 choice of barcode length is largely secondary. Note that this conclusion is robust
660 across 26 datasets and holds for different clustering algorithms.

661 We also find that the choice of species delimitation algorithm matters little for
662 mini-barcodes longer than 200-bp (Fig. 4). This is fortunate as objective clustering

663 and ABGD algorithms are less computationally demanding than PTP, which
664 necessitates the reconstruction of ML trees. However, there are some exceptions.
665 Firstly, when mini-barcodes are extremely short (~100-bp), ABGD and PTP tend to
666 underperform relative to objective clustering. PTP's poor performance for 100-bp
667 mini-barcodes is not surprising given that it relies on tree topologies which cannot be
668 estimated with confidence based on so little data. ABGD's poor performance is
669 mostly observed for certain priors (e.g., P=0.04: Fig. S5 & S6). Under these priors,
670 ABGD tends to lump most of the 100-bp barcodes into one or a few large clusters.
671 Prior-choice also affects ABGD's performance for full-length barcodes. Overall,
672 ABGD does not perform well with very high priors (P = 0.04: Fig. S6 vs. P = 0.001:
673 Fig. 2 & 3) and we conclude that the selection of the best priors and/or clustering
674 thresholds remains a significant challenge for the study of largely unknown faunas
675 that lack morphological or other gene information that can be used as an *a posteriori*
676 criterion for selecting priors/thresholds. In the absence of these data, we would
677 recommend the use of multiple methods and thresholds in order to distinguish robust
678 from labile mOTUs that are heavily dependent on threshold- or prior-choices. The
679 latter mOTUs should be targeted in reconciliation studies utilizing another type of
680 data. As illustrated earlier, these reconciliation studies can focus on only 10-15% of
681 all specimens that cause species-level conflict.

682 *Barcode length and species identification*

683 Similar to our tests of species delimitation, we find that mini-barcodes >200-bp
684 have no significant performance difference when compared with full-length barcodes.
685 Full-length barcodes have only marginally – albeit statistically non-significantly –
686 higher identification success rates than mini-barcodes >200-bp (Table 2: 0.00 –
687 4.15% difference, 0.37% median). This is consistent with the findings of Meusnier et

688 al. (2008) who reported at least 95% identification success for 250-bp barcodes
689 while full-length barcodes performed the best (97% success). Overall, our data
690 suggest that mini-barcodes >200-bp are suitable for species identification. The
691 poorer performance of shorter mini-barcodes (<200-bp) is largely due to an increase
692 of ambiguous matches rather than incorrect matches. These mini-barcodes are less
693 informative which is probably due to their short length and the placement of many
694 short barcodes in a more conserved part of the Folmer region (see below).

695 *Positional effects*

696 Overall, mini-barcodes at the 3' end of the Folmer region outperform mini-
697 barcodes at the 5' end. This is consistent across all three species delimitation
698 methods and was also noticed by Shokralla et al. (2015a) who concluded that mini-
699 barcodes at the 5' end have worse species resolution for fish species. This positional
700 effect is apparent when match ratios are compared across a "sliding window" (Fig.
701 2). The lowest congruence with morphology is observed for 100-bp mini-barcodes
702 with midpoints at the 50-bp, 110-bp and 170-bp marks. However, this positional
703 effect is only significant when the barcode lengths are very short (<200-bp). Once
704 the mini-barcodes are sufficiently long (>200-bp), there is no appreciable difference
705 in performance, which is not surprising because sampling more nucleotides helps
706 with buffering against regional changes in nucleotide variability.

707 These changes in nucleotide variability may have functional reasons related
708 to the conformation of the Cox1 protein in the mitochondrion membrane. The Folmer
709 region of Cox1 contains six transmembrane α- helices that are connected by five
710 loops (Tsukihara et al. 1996; Pentinsaari et al. 2016). Pentinsaari et al. (2016)
711 compared 292 Cox1 sequences across 26 animal phyla and found high amino acid

712 variability in helix I and the loop connecting helix I and helix II (corresponding to
713 position 1-102 of *cox1*), as well as end of helix IV and loop connecting helix IV and V
714 (corresponding to positions ~448-498). These regions of high variability are distant
715 from the active sites and thus less likely to affect Cox1 function (Pentinsaari et al.
716 2016). This may lead to lower selection pressure and thus higher variability in these
717 areas which could impact the performance of mini-barcodes for species delimitation.

718 *Accelerating biodiversity discovery and description*

719 In our study we test whether species discovery with mini-barcodes is as
720 accurate as discovery with full-length barcodes. However, the taxonomic impediment
721 is also caused by the lack of taxonomic capacity for identifying specimens to species
722 and describing new species. Fortunately, the species discovery step can also help
723 with species identification because some specimens placed in mOTUs can be
724 identified via barcode databases. Common species are here more likely to benefit
725 because they are covered by the databases. This is illustrated by our recent work on
726 dragon- and damselflies (Odonata), ants (Formicidae), and non-biting midges
727 (Chironomidae) of Singapore (Baloğlu et al. 2018; Wang et al. 2018; Yeo et al.
728 2018). These studies document why it is important to distinguish between species-
729 and specimen-level identification because the results differ widely. For odonates,
730 BLAST-searches identified more than half of the 95 mOTUs and >75% of the
731 specimens to species. The corresponding numbers for ants and midges were ca.
732 20% and 10% at mOTU-level, and 9% and 40% at the specimen-level; i.e., despite
733 low mOTU identification success for midges, a fairly large number of specimens
734 could be identified because very common species were already represented in a
735 barcode database.

736 In addition, mOTUs are also useful for understanding biodiversity patterns
737 because they can be readily compared across studies and borders (Ratnasingham
738 and Hebert 2013). In contrast, a new species identified based on morphology usually
739 remains unavailable to the scientific community until the descriptions are published
740 unless associated molecular information is also present. This is a very significant
741 difference because a large amount of downstream biodiversity analysis can be
742 carried out based on newly discovered species regardless of whether they are were
743 discovered with morphological or molecular means. However, cross-study
744 comparisons are only straightforward for mOTUs because sequences are readily
745 shared and compared. This allows for the study of species richness and abundances
746 before taxa are described. Even studies covering different time periods can be
747 carried out, which is increasingly important in the 21st century.

748 *Conclusions*

749 We here illustrate that mini-barcodes are as reliable for pre-sorting specimens
750 into putative species as full-length barcodes. Mini-barcodes are also suitable for
751 identifying unidentified barcodes to species based on barcode reference databases.
752 We would thus argue that mini-barcodes should be preferred over full-length
753 barcodes because (1) they can be obtained more readily for specimens that only
754 contain degraded DNA (Hajibabaei et al. 2006) and (2) are much more cost-
755 effective. In particular, we recommend the use of mini-barcodes >200-bp at the 3'
756 end of the Folmer region. It is encouraging that such mini-barcodes perform well
757 across a large range of metazoan taxa. These conclusions are based on three
758 species delimitation algorithms (objective clustering, ABGD and PTP) which, overall,
759 have no appreciable effect on the performance of barcodes. If the DNA of the
760 specimens is so degraded that very short mini-barcodes have to be obtained, we

761 advise against the use of PTP and ABGD (especially with high priors) in order to
762 reduce the likelihood that morphospecies are lumped.

763

764 **Funding**

765 This work was supported by a Ministry of Education grant on biodiversity discovery
766 (R-154-000-A22-112).

767

768 **Acknowledgements**

769 We would like to acknowledge Athira Adom and Jonathan Ho for data processing,
770 Lee Wan Ting for performing the molecular work and Emily Hartop and Wendy Wang
771 for commenting on the manuscript.

772

773 **References**

774 Ahrens D., Fujisawa T., Krammer H.-J., Eberle J., Fabrizi S., Vogler A.P. 2016.
775 Rarity and incomplete sampling in DNA-based species delimitation. Syst. Biol.
776 65:478–494.

777 Ang Y., Meier R., Su K.F.-Y., Rajaratnam G. 2017. Hidden in the urban parks of New
778 York City: Themira lohmanus, a new species of Sepsidae described based on
779 morphology, DNA sequences, mating behavior, and reproductive isolation
780 (Sepsidae, Diptera). ZooKeys. 698:95–111.

781 Baldwin C., Castillo C., Weigt L., Victor B. 2011. Seven new species within western
782 Atlantic Starksia atlantica, S. lepicoelia, and S. sluiteri (Teleostei,
783 Labrisomidae), with comments on congruence of DNA barcodes and species.
784 ZooKeys. 79:21–72.

785 Ball S.L., Hebert P.D.N., Burian S.K., Webb J.M. 2005. Biological identifications of
786 mayflies (Ephemeroptera) using DNA barcodes. J. North Am. Benthol. Soc.
787 24:508–524.

788 Baloğlu B., Clews E., Meier R. 2018. NGS barcoding reveals high resistance of a
789 hyperdiverse chironomid (Diptera) swamp fauna against invasion from
790 adjacent freshwater reservoirs. Front. Zool. 15:31.

791 Bar-On Y.M., Phillips R., Milo R. 2018. The biomass distribution on Earth. Proc. Natl.
792 Acad. Sci. 115:6506–6511.

793 Bates D., Mächler M., Bolker B., Walker S. 2014. Fitting linear mixed-effects models
794 using *lme4*. ArXiv14065823 Stat.

795 Bi K., Linderoth T., Vanderpool D., Good J.M., Nielsen R., Moritz C. 2013. Unlocking
796 the vault: next-generation museum population genomics. Mol. Ecol. 22:6018–
797 6032.

798 Bickel D.J. 1999. What museum collections reveal about species accumulation,
799 richness, and rarity: an example from the Diptera. The other. 99:174–181.

800 Blaimer B.B., Lloyd M.W., Guillory W.X., Brady S.G. 2016. Sequence capture and
801 phylogenetic utility of genomic ultraconserved elements obtained from pinned
802 insect specimens. PLoS ONE. 11:e0161531.

803 Burns J.M., Janzen D.H., Merhdad Hajibabai, Winnie Hallwachs, Paul D. N. Hebert.
804 2007. DNA barcodes of closely related (but morphologically and ecologically
805 distinct) species of skipper butterflies (Hesperiidae) can differ by only one to
806 three nucleotides. J. Lepidopterists' Soc. 61:138–153.

807 Cafaro P. 2015. Three ways to think about the sixth mass extinction. Biol. Conserv.
808 192:387–393.

809 Ceballos G., Ehrlich P.R., Barnosky A.D., García A., Pringle R.M., Palmer T.M.
810 2015. Accelerated modern human–induced species losses: Entering the sixth
811 mass extinction. Sci. Adv. 1:e1400253.

812 Chase M.W., Fay M.F. 2009. Barcoding of plants and fungi. Science. 325:682–683.

813 Cooper A. 1994. DNA from museum specimens. In: Herrmann B., Hummel S.,
814 editors. Ancient DNA: Recovery and Analysis of Genetic Material from
815 Paleontological, Archaeological, Museum, Medical, and Forensic Specimens.
816 New York, NY: Springer New York. p. 149–165.

817 Cywinska A., Hunter F.F., Hebert P.D.N. 2006. Identifying Canadian mosquito
818 species through DNA barcodes. Med. Vet. Entomol. 20:413–424.

819 Dayrat B. 2005. Towards integrative taxonomy. Biol. J. Linn. Soc. 85:407–415.

820 Deagle B.E., Eveson J.P., Jarman S.N. 2006. Quantification of damage in DNA
821 recovered from highly degraded samples – a case study on DNA in faeces.
822 Front. Zool. 3:11.

823 Decru E., Moelants T., De Gelas K., Vreven E., Verheyen E., Snoeks J. 2016.
824 Taxonomic challenges in freshwater fishes: a mismatch between morphology

825 and DNA barcoding in fish of the north-eastern part of the Congo basin. Mol.
826 Ecol. Resour. 16:342–352.

827 Dincă V., Montagud S., Talavera G., Hernández-Roldán J., Munguira M.L., García-
828 Barros E., Hebert P.D.N., Vila R. 2015. DNA barcode reference library for
829 Iberian butterflies enables a continental-scale preview of potential cryptic
830 diversity. Sci. Rep. 5:12395.

831 Ermakov O.A., Simonov E., Surin V.L., Titov S.V., Brandler O.V., Ivanova N.V.,
832 Borisenko A.V. 2015. Implications of hybridization, NUMTs, and overlooked
833 diversity for DNA barcoding of Eurasian ground squirrels. PLoS ONE.
834 10:e0117201.

835 Fagan-Jeffries E.P., Cooper S.J.B., Bertozzi T., Bradford T.M., Austin A.D. 2018.
836 DNA barcoding of microgastrine parasitoid wasps (Hymenoptera: Braconidae)
837 using high-throughput methods more than doubles the number of species
838 known for Australia. Mol. Ecol. Resour. 18:1132–1143.

839 Ficetola G.F., Miaud C., Pompanon F., Taberlet P. 2008. Species detection using
840 environmental DNA from water samples. Biol. Lett. 4:423–425.

841 Folmer O., Black M., Hoeh W., Lutz R., Vrijenhoek R. 1994. DNA primers for
842 amplification of mitochondrial cytochrome c oxidase subunit I from diverse
843 metazoan invertebrates. Mol. Mar. Biol. Biotechnol. 3:294–299.

844 Franz N.M. 2005. On the lack of good scientific reasons for the growing
845 phylogeny/classification gap. Cladistics. 21:495–500.

846 Guschanski K., Krause J., Sawyer S., Valente L.M., Bailey S., Finstermeier K., Sabin
847 R., Gilissen E., Sonet G., Nagy Z.T., Lenglet G., Mayer F., Savolainen V.
848 2013. Next-generation museomics disentangles one of the largest primate
849 radiations. Syst. Biol. 62:539–554.

850 Hajibabaei M., McKenna C. 2012. DNA Mini-barcodes. In: Kress W.J., Erickson D.L.,
851 editors. DNA Barcodes. Totowa, NJ: Humana Press. p. 339–353.

852 Hajibabaei M., Smith M.A., Janzen D.H., Rodriguez J.J., Whitfield J.B., Hebert
853 P.D.N. 2006. A minimalist barcode can identify a specimen whose DNA is
854 degraded. Mol. Ecol. Notes. 6:959–964.

855 Han T., Lee W., Lee S., Park I.G., Park H. 2016. Reassessment of species diversity
856 of the subfamily Denticollinae (Coleoptera: Elateridae) through DNA
857 barcoding. PLoS ONE. 11:e0148602.

858 Hebert P.D.N., Braukmann T.W.A., Prosser S.W.J., Ratnasingham S., deWaard
859 J.R., Ivanova N.V., Janzen D.H., Hallwachs W., Naik S., Sones J.E.,
860 Zakharov E.V. 2018. A Sequel to Sanger: amplicon sequencing that scales.
861 BMC Genomics. 19:219.

862 Hebert P.D.N., Cywinska A., Ball S.L., deWaard J.R. 2003. Biological identifications
863 through DNA barcodes. Proc. R. Soc. Lond. B Biol. Sci. 270:313–321.

Hollatz C., Leite B.R., Lobo J., Froufe H., Egas C., Costa F.O. 2016. Priming of a DNA metabarcoding approach for species identification and inventory in marine macrobenthic communities. Genome. 60:260–271.

Hollingsworth P.M., Graham S.W., Little D.P. 2011. Choosing and using a plant DNA barcode. PLoS ONE. 6:e19254.

Huang D., Meier R., Todd P.A., Chou L.M. 2008. Slow mitochondrial COI sequence evolution at the base of the Metazoan tree and its implications for DNA barcoding. J. Mol. Evol. 66:167–174.

Jones M., Ghoorah A., Blaxter M. 2011. jMOTU and Taxonerator: Turning DNA barcode sequences into annotated operational taxonomic units. PLoS ONE. 6:e19259.

Kapli P., Lutteropp S., Zhang J., Kobert K., Pavlidis P., Stamatakis A., Flouri T. 2017. Multi-rate Poisson Tree Processes for single-locus species delimitation under Maximum Likelihood and Markov Chain Monte Carlo. Bioinformatics.:btx025.

Katoh K., Standley D.M. 2013. MAFFT multiple sequence alignment software version 7: Improvements in performance and usability. Mol. Biol. Evol. 30:772–780.

Kemp C. 2015. The billions of specimens in natural-history museums are becoming more useful for tracking Earth's shrinking biodiversity. But the collections also face grave threats. Nat. News. 518:292–294.

Krell F.-T. 2004. Parataxonomy vs. taxonomy in biodiversity studies – pitfalls and applicability of 'morphospecies' sorting. Biodivers. Conserv. 13:795–812.

Landi M., Dimech M., Arculeo M., Biondo G., Martins R., Carneiro M., Carvalho G.R., Brutto S.L., Costa F.O. 2014. DNA Barcoding for species assignment: The case of mediterranean marine fishes. PLoS ONE. 9:e106135.

Lenth R. 2018. Emmeans: Estimated marginal means. Aka Least-Sq. Means R.

Leray M., Yang J.Y., Meyer C.P., Mills S.C., Agudelo N., Ranwez V., Boehm J.T., Machida R.J. 2013. A new versatile primer set targeting a short fragment of the mitochondrial COI region for metabarcoding metazoan diversity: application for characterizing coral reef fish gut contents. Front. Zool. 10:34.

Lim N.K.M., Tay Y.C., Srivathsan A., Tan J.W.T., Kwik J.T.B., Baloğlu B., Meier R., Yeo D.C.J. 2016. Next-generation freshwater bioassessment: eDNA metabarcoding with a conserved metazoan primer reveals species-rich and reservoir-specific communities. R. Soc. Open Sci. 3:160635.

Lister A.M., Stephen J. Brooks, Phillip B. Fenberg, Adrian G. Glover, Karen E. James, Kenneth G. Johnson, Ellinor Michel, Beth Okamura, Mark Spencer, John R. Stewart, Jonathan A. Todd, Eugenia Valsami-Jones, Jeremy Young. 2011. Natural history collections as sources of long-term datasets. Trends Ecol. Evol. 26:153–154.

902 Meier R. 2008. DNA sequences in taxonomy, opportunities and challenges. New
903 Taxon.:65–127.

904 Meier R. 2017. Citation of taxonomic publications: the why, when, what and what
905 not: Species citations. Syst. Entomol. 42:301–304.

906 Meier R., Shiyang K., Vaidya G., Ng P.K.L. 2006. DNA barcoding and taxonomy in
907 Diptera: A tale of high intraspecific variability and low identification success.
908 Syst. Biol. 55:715–728.

909 Meier R., Wong W., Srivathsan A., Foo M. 2016. $1 DNA barcodes for reconstructing
910 complex phenomes and finding rare species in specimen-rich samples.
911 Cladistics. 32:100–110.

912 Meusnier I., Singer G.A., Landry J.-F., Hickey D.A., Hebert P.D., Hajibabaei M. 2008.
913 A universal DNA mini-barcode for biodiversity analysis. BMC Genomics.
914 9:214.

915 Min X.J., Hickey D.A. 2007. Assessing the effect of varying sequence length on DNA
916 barcoding of fungi. Mol. Ecol. Notes. 7:365–373.

917 Mioduchowska M., Czyż M.J., Gołdyn B., Kur J., Sell J. 2018. Instances of erroneous
918 DNA barcoding of metazoan invertebrates: Are universal cox1 gene primers
919 too “universal”? PLOS ONE. 13:e0199609.

920 Morinière J., Balke M., Doczkal D., Geiger M.F., Hardulak L.A., Haszprunar G.,
921 Hausmann A., Hendrich L., Regalado L., Rulik B., Schmidt S., Wägele J.,
922 Hebert P.D.N. 2019. A DNA barcode library for 5,200 German flies and
923 midges (Insecta: Diptera) and its implications for metabarcoding-based
924 biomonitoring. Mol. Ecol. Resour. 19:900–928.

925 Pentinsaari M., Salmela H., Mutanen M., Roslin T. 2016. Molecular evolution of a
926 widely-adopted taxonomic marker (COI) across the animal tree of life. Sci.
927 Rep. 6:35275.

928 Puillandre N., Lambert A., Brouillet S., Achaz G. 2012. ABGD, Automatic Barcode
929 Gap Discovery for primary species delimitation. Mol. Ecol. 21:1864–1877.

930 Ratnasingham S., Hebert P.D.N. 2013. A DNA-based registry for all animal species:
931 the Barcode Index Number (BIN) system. PLoS ONE. 8:e66213.

932 Renaud A.K., Savage J., Adamowicz S.J. 2012. DNA barcoding of Northern Nearctic
933 Muscidae (Diptera) reveals high correspondence between morphological and
934 molecular species limits. BMC Ecol. 12:24.

935 Riedel A., Daawia D., Balke M. 2010. Deep *cox1* divergence and hyperdiversity of
936 *Trigonopterus* weevils in a New Guinea mountain range (Coleoptera,
937 Curculionidae). Zool. Scr. 39:63–74.

938 Roe A.D., Sperling F.A.H. 2007. Patterns of evolution of mitochondrial cytochrome c
939 oxidase I and II DNA and implications for DNA barcoding. Mol. Phylogenet.
940 Evol. 44:325–345.

941 Roskov Y., Abucay L., Orrell T., Nicolson D., Bailly N., Kirk P.M., Bourgoin T.,
942 DeWalt R.E., Decock W., De Wever A. 2018. Species 2000 & ITIS Catalogue
943 of Life. 2017, Annual Checklist. Digital resource at www. catalogueoflife.
944 org/annual-checklist/2017. Species 2000: Naturalis, Leiden, the Netherlands.
945 ISSN 2405-884X. .

946 Rubinoff D., Cameron S., Will K. 2006. A genomic perspective on the shortcomings
947 of mitochondrial DNA for “Barcoding” identification. J. Hered. 97:581–594.

948 Sánchez-Bayo F., Wyckhuys K.A.G. 2019. Worldwide decline of the entomofauna: A
949 review of its drivers. Biol. Conserv. 232:8–27.

950 Schlick-Steiner B.C., Steiner F.M., Seifert B., Stauffer C., Christian E., Crozier R.H.
951 2010. Integrative Taxonomy: A Multisource Approach to Exploring
952 Biodiversity. Annu. Rev. Entomol. 55:421–438.

953 Shokralla S., Hellberg R.S., Handy S.M., King I., Hajibabaei M. 2015a. A DNA mini-
954 barcoding system for authentication of processed fish products. Sci. Rep.
955 5:15894.

956 Shokralla S., Porter T.M., Gibson J.F., Dobosz R., Janzen D.H., Hallwachs W.,
957 Golding G.B., Hajibabaei M. 2015b. Massively parallel multiplex DNA
958 sequencing for specimen identification using an Illumina MiSeq platform. Sci.
959 Rep. 5:9687.

960 Smith M.A., Rodriguez J.J., Whitfield J.B., Deans A.R., Janzen D.H., Hallwachs W.,
961 Hebert P.D.N. 2008. Extreme diversity of tropical parasitoid wasps exposed
962 by iterative integration of natural history, DNA barcoding, morphology, and
963 collections. Proc. Natl. Acad. Sci. 105:12359–12364.

964 Srivathsan A., Baloğlu B., Wang W., Tan W.X., Bertrand D., Ng A.H.Q., Boey E.J.H.,
965 Koh J.J.Y., Nagarajan N., Meier R. 2018. A MinION™-based pipeline for fast
966 and cost-effective DNA barcoding. Mol. Ecol. Resour. 18:1035–1049.

967 Srivathsan A., Hartop E., Puniamoorthy J., Lee W.T., Kutty S.N., Kurina O., Meier R.
968 2019. 1D MinION sequencing for large-scale species discovery: 7000 scuttle
969 flies (Diptera: Phoridae) from one site in Kibale National Park (Uganda)
970 revealed to belong to >650 species. bioRxiv.:622365.

971 Srivathsan A., Meier R. 2012. On the inappropriate use of Kimura-2-parameter (K2P)
972 divergences in the DNA-barcoding literature. Cladistics. 28:190–194.

973 Stamatakis A. 2014. RAxML version 8: a tool for phylogenetic analysis and post-
974 analysis of large phylogenies. Bioinformatics. 30:1312–1313.

975 Stork N.E. 2018. How many species of insects and other terrestrial arthropods are
976 there on Earth? Annu. Rev. Entomol. 63:31–45.

977 Stork N.E., McBroom J., Gely C., Hamilton A.J. 2015. New approaches narrow
978 global species estimates for beetles, insects, and terrestrial arthropods. Proc.
979 Natl. Acad. Sci. 112:7519–7523.

980 Sultana S., Ali Md.E., Hossain M.A.M., Asing, Naquiah N., Zaidul I.S.M. 2018.
981 Universal mini COI barcode for the identification of fish species in processed
982 products. Food Res. Int. 105:19–28.

983 Tamura K., Stecher G., Peterson D., Filipski A., Kumar S. 2013. MEGA6: molecular
984 evolutionary genetics analysis version 6.0. Mol. Biol. Evol. 30:2725–2729.

985 Tan D.S.H., Ang Y., Lim G.S., Ismail M.R.B., Meier R. 2010. From 'cryptic species' to
986 integrative taxonomy: an iterative process involving DNA sequences,
987 morphology, and behaviour leads to the resurrection of *Sepsis pyrrhosoma*
988 (Sepsidae: Diptera). Zool. Scr. 39:51–61.

989 Taylor H.R., Harris W.E. 2012. An emergent science on the brink of irrelevance: a
990 review of the past 8 years of DNA barcoding. Mol. Ecol. Resour. 12:377–388.

991 Tsukihara T., Aoyama H., Yamashita E., Tomizaki T., Yamaguchi H., Shinzawa-Itoh
992 K., Nakashima R., Yaono R., Yoshikawa S. 1996. The whole structure of the
993 13-subunit oxidized cytochrome c oxidase at 2.8 Å. Science. 272:1136–1144.

994 Valan M., Makonyi K., Maki A., Vondráček D., Ronquist F. 2019. Automated
995 taxonomic identification of insects with expert-level accuracy using effective
996 feature transfer from convolutional networks. Syst. Biol. 0:1–20.

997 Wang W.Y., Srivathsan A., Foo M., Yamane S.K., Meier R. 2018. Sorting specimen-
998 rich invertebrate samples with cost-effective NGS barcodes: Validating a
999 reverse workflow for specimen processing. Mol. Ecol. Resour. 18:490–501.

1000 Will K.W., Rubinoff D. 2004. Myth of the molecule: DNA barcodes for species cannot
1001 replace morphology for identification and classification. Cladistics. 20:47–55.

1002 Yang C., Tan S., Meng G., Bourne D.G., O'Brien P.A., Xu J., Liao S., Chen A., Chen
1003 X., Liu S. 2018. Access COI barcode efficiently using high throughput Single-
1004 End 400 bp sequencing. .

1005 Yang Z., Rannala B. 2010. Bayesian species delimitation using multilocus sequence
1006 data. Proc. Natl. Acad. Sci. 107:9264–9269.

1007 Yeates D.K., Zwick A., Mikheyev A.S. 2016. Museums are biobanks: unlocking the
1008 genetic potential of the three billion specimens in the world's biological
1009 collections. Curr. Opin. Insect Sci. 18:83–88.

1010 Yeo D., Puniamoorthy J., Ngiam R.W.J., Meier R. 2018. Towards holomorphology in
1011 entomology: rapid and cost-effective adult-larva matching using NGS
1012 barcodes: Life-history stage matching with NGS barcodes. Syst. Entomol.
1013 43:678–691.

1014 Yu H.J., You Z.H. 2010. Comparison of DNA truncated barcodes and full-barcodes
1015 for species identification. Int. Conf. Intell. Comput.:108–114.

1016 Zhang J., Kapli P., Pavlidis P., Stamatakis A. 2013. A general species delimitation
1017 method with applications to phylogenetic placements. Bioinformatics.
1018 29:2869–2876.

1019

1020 **Figure Captions**

1021 **Table 1.** Proportion of specimens congruent between morphospecies and mOTU
1022 clusters (20 empirical datasets/6 clade-based datasets) under the three stringency
1023 classes. Values in brackets represent an upper bound estimate of number of
1024 specimens causing conflict.

1025 **Table 2.** Proportion of correct/incorrect/ambiguous/unidentified specimens in the
1026 "best close match" analysis.

1027 **Figure 1.** Positions of the mini-barcodes with established primers assessed in this
1028 study.

1029 **Figure 2.** Performance of mini-barcodes along a sliding window (100-bp, 200-bp,
1030 300-bp). Mini-barcode position is indicated on the x-axis and congruence with
1031 morphology on the y-axis. mOTUs were obtained with Objective Clustering (2%),
1032 ABGD P=0.001 prior), and PTP. Each line represents one data set while the boxplots
1033 summarise the values across datasets. Significant deviations from the results
1034 obtained with full-length barcodes are indicated with color-coded asterisks (* = $p <$
1035 0.05; ** = $p < 0.001$; red = poorer and green = higher congruence with morphology).

1036 **Figure 3.** Match ratios across three different species delimitation methods. Mini-
1037 barcodes (columns) are sorted by primer length while the 20 empirical datasets
1038 (rows) are sorted by average match ratio. The six clade-specific datasets from
1039 GenBank are grouped below. Match ratios above average are coloured green, while
1040 those below average are in pink. The highest match ratio values are indicated with
1041 white text.

1042 **Figure 4.** Comparison of species delimitation methods for full-length and mini-
1043 barcodes generated by "sliding windows" (100-bp, 200-bp, 300-bp).

1044 **Figure 5.** Proportion of conserved sites along the full-length barcode (sliding

1045 windows of 100-bp, 200-bp, 300-bp).

1046 **Table 1.** Proportion of specimens congruent between morphospecies and mOTU clusters (20 empirical datasets/6 clade-based
1047 datasets) under the three stringency classes. Values in brackets represent an upper bound estimate of number of specimens causing
1048 conflict.

				Objective clustering, 2% p-distance			
Length	**295**	**307**	**313**	**407**	**657**	**Average**	**Median**
Midpoint	**405**	**154**	**502**	**455**	**329**		
Class I	77/57% (7475/41367)	76/56% (7511/42052)	77/57% (7275/40857)	77/57% (7246/40849)	77/58% (7118/40327)	77/57% (7325/41090)	77/57% (7372/40941)
Class II	90/75% (3283/23846)	90/75% (3333/24794)	90/75% (3131/23554)	90/76% (3078/23304)	90/76% (3006/23349)	90/75% (3166/23769)	90/76% (3112/23469)
Class III	91/82% (3021/17875)	91/81% (2954/18981)	91/82% (2822/17666)	91/82% (2813/17511)	91/82% (2759/17509)	91/82% (2874/17908)	91/82% (2862/17745)
				ABGD, P=0.001			
Length	**295**	**307**	**313**	**407**	**657**	**Average**	**Median**
Midpoint	**405**	**154**	**502**	**455**	**329**		
Class I	75/55% (7916/42576)	76/55% (7685/42403)	75/55% (8169/42787)	73/53% (8583/45131)	69/47% (9833/49848)	74/53% (8437/44549)	74/54% (8126/43386)
Class II	89/75% (3305/24555)	89/75% (3442/24541)	89/75% (3336/24267)	89/74% (3526/25153)	88/72% (3901/26691)	89/74% (3502/25041)	89/74% (3382/24625)
Class III	91/81% (2981/18303)	91/81% (2906/18509)	90/81% (2984/18352)	90/80% (3041/18978)	89/78% (3482/20860)	90/80% (3079/19000)	91/81% (2927/18494)
				PTP			
Length	**295**	**307**	**313**	**407**	**657**	**Average**	**Median**
Midpoint	**405**	**154**	**502**	**455**	**329**		
Class I	76/57% (7643/40692)	76/56% (7744/42608)	77/57% (7369/41588)	78/57% (7130/41056)	78/58% (7207/40234)	77/57% (7419/41236)	77/57% (7318/40839)
Class II	89/75% (3322/23946)	89/75% (3549/24598)	90/75% (3230/23857)	90/76% (3109/23583)	90/76% (3127/22912)	90/75% (3267/23779)	90/76% (3198/23659)
Class III	90/81% (3091/18208)	90/81% (3334/19189)	91/82% (2926/18179)	91/81% (2813/18968)	91/82% (2859/17317)	91/81% (3005/18372)	91/81% (2937/18193)

1049

1050 **Table 2.** Proportion of correct/incorrect/ambiguous/unidentified specimens in the "best close match" analysis.

	Published Primers									
Dataset	**94**	**130**	**145**	**164**	**189**	**295**	**307**	**313**	**407**	**657**
Great Barrier Reef Fish	85/1/0/15	83/1/3/13	83/1/2/14	85/0/0/14	86/1/0/13	86/0/0/14	85/1/0/14	86/0/0/14	86/0/0/14	86/0/0/14
South China Sea Fish	93/0/1/6	91/1/3/6	91/1/3/6	93/0/1/6	93/0/1/6	94/0/0/6	93/0/1/6	93/1/1/6	94/1/0/6	94/0/0/6
North Sea Molluscs	90/0/0/10	91/0/0/9	92/0/0/8	92/0/0/8	92/0/0/8	92/0/0/8	92/0/0/8	91/0/0/9	91/0/0/9	92/0/0/8
Canadian Echinoderms	95/0/0/5	95/0/0/4	95/0/0/5	96/0/0/4	96/0/0/4	95/0/0/5	96/0/0/4	95/0/0/5	96/0/0/4	96/0/0/4
Ecuadorian Geometridae	84/0/0/15	85/1/0/13	85/0/0/14	85/0/0/14	85/0/0/14	86/0/0/14	86/0/0/14	86/0/0/14	86/0/0/14	86/0/0/14
German Aranea & Opiliones	88/0/5/7	89/0/5/5	89/0/5/6	90/1/4/5	90/0/4/5	92/0/2/6	91/1/3/5	92/0/2/5	92/1/2/5	93/1/2/5
European Marine Fish	92/0/7/1	91/0/7/1	92/0/6/2	96/0/3/1	96/0/3/1	97/0/1/1	97/0/1/1	96/0/2/1	97/0/1/1	98/0/1/1
South American Butterflies	89/0/4/7	91/1/2/6	92/0/1/6	92/0/1/6	93/0/0/6	93/0/0/6	94/0/0/6	94/0/0/6	94/0/0/6	94/0/0/6
German EPT	92/0/1/7	93/0/1/5	94/0/1/6	94/0/0/6	94/0/0/6	93/0/0/6	94/0/0/5	94/0/0/6	94/0/0/6	94/0/0/6
Northwest Pacific Molluscs	69/2/15/14	75/2/10/13	74/2/10/13	73/2/12/12	73/2/12/12	77/2/8/12	77/2/9/12	76/3/9/12	77/3/8/12	78/4/6/12
Amazonian Moths	62/2/1/36	63/3/1/34	63/3/1/34	62/2/1/35	63/2/1/35	63/1/1/35	63/2/1/34	63/1/1/35	63/1/1/35	63/2/1/34
North American Birds	77/1/11/11	72/2/15/10	73/2/15/11	81/2/7/10	80/1/9/10	83/2/5/11	81/2/6/11	84/2/3/10	85/2/3/10	85/2/2/11
French Guianan Earthworms	96/0/0/4	97/0/0/3	97/0/0/3	96/0/0/4	96/0/0/4	97/0/0/3	97/0/0/3	97/0/0/3	97/0/0/3	96/0/0/4
Pakistani Lepidoptera	88/1/3/8	90/1/1/8	90/1/1/8	91/1/1/8	91/1/0/8	91/0/0/8	91/0/0/8	91/0/0/8	91/0/0/8	91/0/0/8
Tanytarsus	81/1/5/12	83/2/5/11	82/2/5/12	86/2/2/11	85/2/3/10	83/2/3/12	86/2/3/9	85/2/2/10	86/2/1/11	87/2/1/11
North European Tachinidae	64/2/14/19	65/3/16/17	65/3/15/17	66/3/13/18	65/3/15/17	67/3/11/18	68/3/12/17	68/3/10/18	69/3/10/18	71/4/8/17
Congolese Fish	80/1/10/9	78/1/11/9	79/1/11/10	84/2/6/7	86/2/5/7	85/2/5/8	86/2/4/8	86/3/4/7	86/3/4/7	88/3/2/7
North American Pyraustinae	93/1/4/3	94/1/4/1	96/1/2/1	96/1/1/2	97/0/0/2	97/0/0/3	98/1/0/2	97/0/0/3	97/0/0/2	98/2/0/2
Ecuadorian Chrysomelidae	74/0/1/25	76/0/1/23	76/0/1/23	76/0/1/23	76/0/1/24	75/0/1/24	76/0/1/23	75/0/1/24	75/0/1/24	75/0/1/24
Iberian Butterflies	77/0/22/1	85/0/15/0	86/0/13/0	87/0/12/0	89/0/10/0	93/0/6/0	94/1/5/0	94/0/5/0	96/0/4/0	97/1/3/0

1051

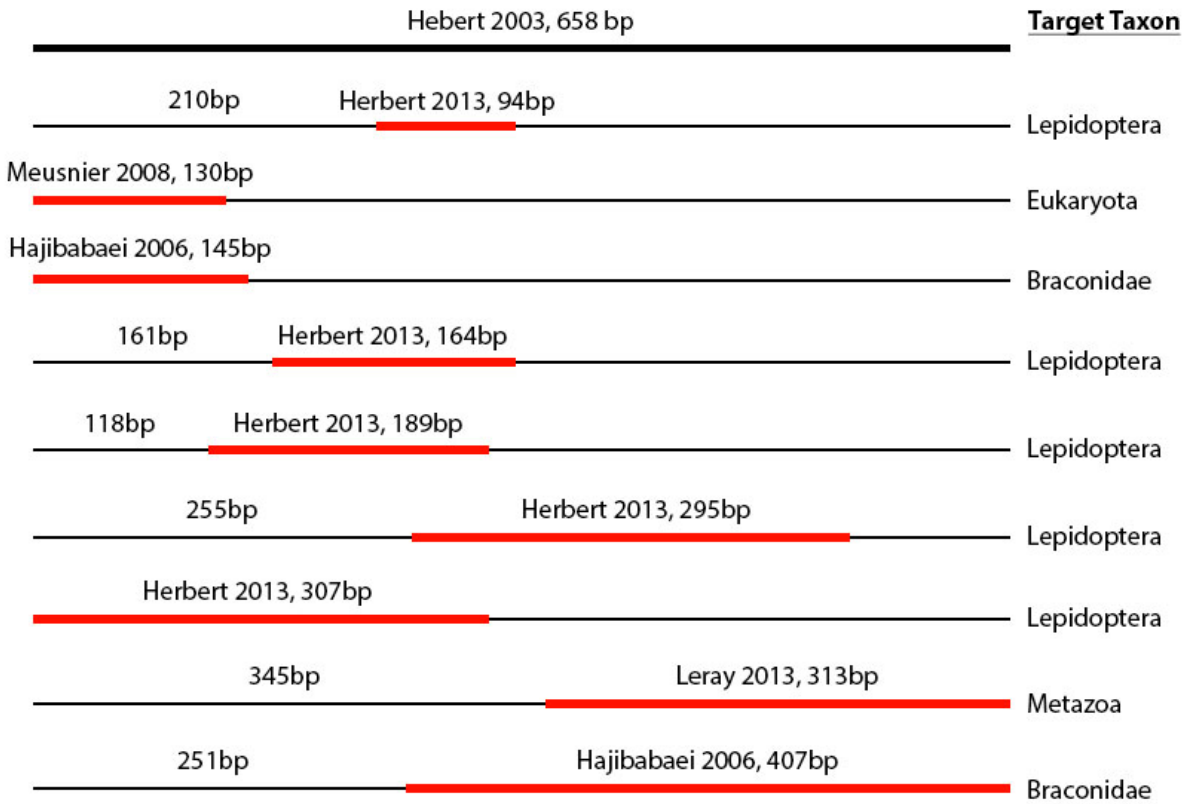

Figure 1. Positions of the mini-barcodes with established primers assessed in this study.

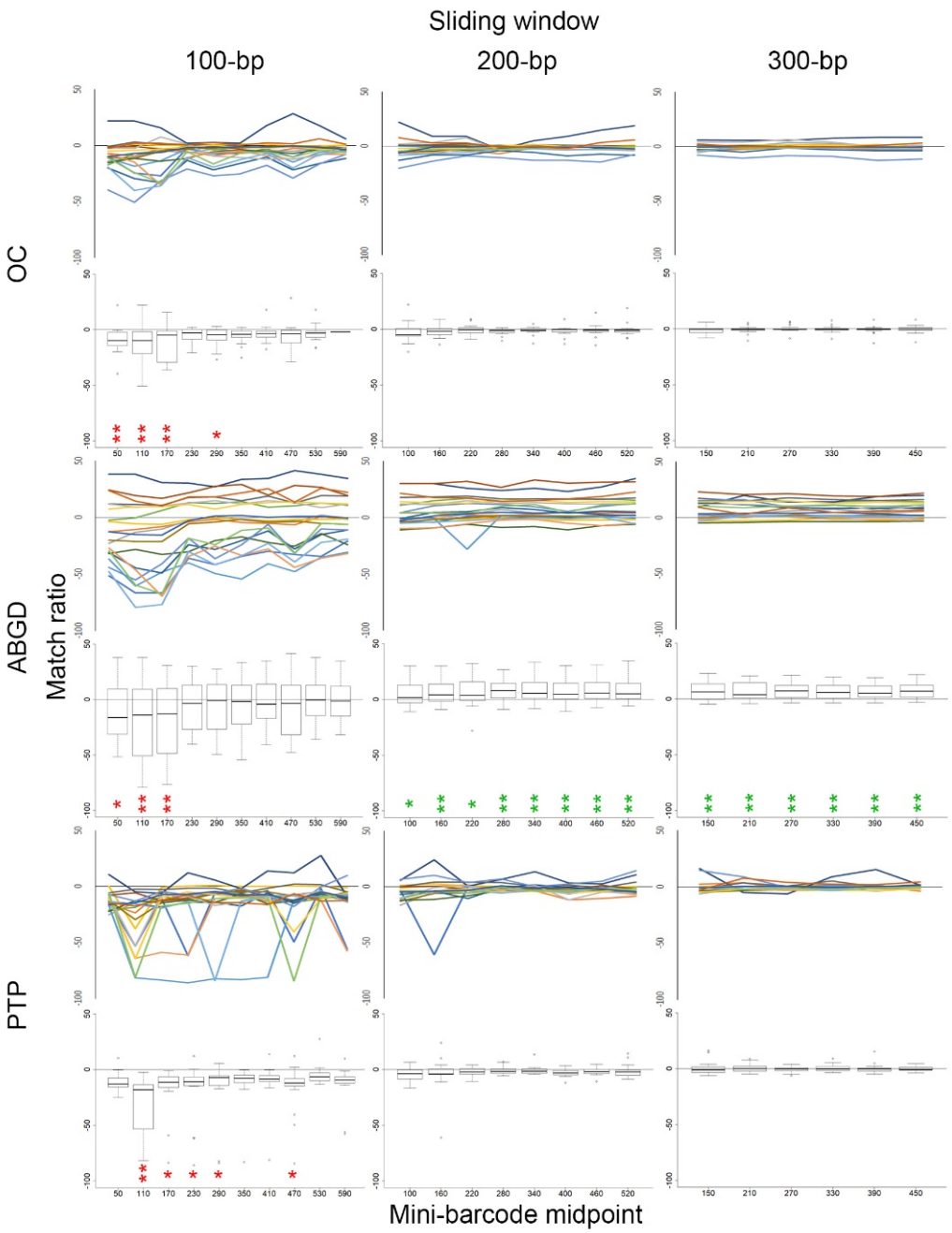

1055

1056 **Figure 2.** Performance of mini-barcodes along a sliding window (100-bp, 200-bp,
1057 300-bp). Mini-barcode position is indicated on the x-axis and congruence with
1058 morphology on the y-axis. mOTUs were obtained with Objective Clustering (2%),
1059 ABGD P=0.001 prior), and PTP. Each line represents one data set while the boxplots
1060 summarise the values across datasets. Significant deviations from the results
1061 obtained with full-length barcodes are indicated with color-coded asterisks (* = p <
1062 0.05; ** = p < 0.001; red = poorer and green = higher congruence with morphology).

Objective clustering 2%

Length	94	130	145	164	189	295	307	313	407	657	Average
Midpoint	**257**	**65**	**73**	**243**	**213**	**405**	**154**	**502**	**455**	**329**	
20 Empirical Datasets											
Ecuadorian Geometridae	94	95	96	98	98	99	99	99	99	99	98
Great Barrier Reef Fish	94	91	92	95	95	97	94	97	97	97	95
Pakistani Lepidoptera	88	87	90	91	91	95	93	95	95	97	92
South China Sea Fish	92	86	88	94	94	94	94	94	94	95	92
South American Butterflies	83	89	88	90	90	92	93	92	93	93	90
Amazonian Moths	87	88	89	90	91	91	90	91	91	91	90
European Marine Fish	81	74	84	92	90	97	93	94	97	97	90
Canadian Echinoderms	81	89	85	91	88	91	91	91	94	95	90
North Sea Molluscs	77	85	84	90	90	89	92	84	85	87	86
German EPT	78	85	84	85	84	83	85	83	83	84	83
North European Tachinidae	81	81	82	81	83	83	83	83	83	84	82
North American Birds	84	77	77	82	81	85	82	84	85	85	82
German Aranea & Opiliones	69	77	76	79	78	80	82	82	80	81	78
Northwest Pacific Molluscs	72	74	73	77	77	78	77	77	78	78	76
North American Pyraustinae	61	56	64	69	77	74	75	78	77	84	71
Congolese Fish	63	61	60	68	70	72	66	70	71	70	67
French Guianan Earthworms	52	74	74	54	63	65	65	65	65	60	64
Iberian Butterflies	51	55	56	59	63	61	62	63	61	65	60
Ecuadorian Chrysomelidae	54	54	55	55	56	55	55	55	55	55	55
Tanytarsus	47	51	49	57	57	58	59	55	56	57	55
Consolidated:	**77**	**78**	**79**	**82**	**82**	**83**	**83**	**83**	**83**	**84**	**81**
6 Clade-based Datasets											
Coleoptera	76	78	78	80	80	80	81	80	80	81	79
Lepidoptera	72	73	74	77	78	80	79	80	81	81	78
Diptera	72	74	74	76	76	77	78	76	77	77	76
Arachnida	63	66	65	65	66	68	68	67	67	67	66
Actinopterygii	64	60	61	65	65	66	64	66	66	66	64
Hymenoptera	60	63	63	63	63	65	65	65	64	64	64
Consolidated:	**69**	**70**	**70**	**72**	**73**	**74**	**73**	**73**	**73**	**74**	**72**
Overall Consolidated:	**70**	**72**	**72**	**74**	**75**	**76**	**75**	**75**	**75**	**76**	**74**

ABGD P=0.001

Length	94	130	145	164	189	295	307	313	407	657	Average
Midpoint	**257**	**65**	**73**	**243**	**213**	**405**	**154**	**502**	**455**	**329**	
20 Empirical Datasets											
North Sea Molluscs	94	90	92	94	94	89	90	89	86	80	90
South China Sea Fish	92	78	83	89	93	94	92	93	91	90	89
Great Barrier Reef Fish	79	75	79	90	89	97	92	95	95	94	88
Canadian Echinoderms	87	78	76	91	91	87	91	95	92	89	88
Pakistani Lepidoptera	61	67	75	84	89	95	91	95	96	94	85
German EPT	85	84	85	86	87	83	85	84	78	67	82
Ecuadorian Geometridae	48	58	57	96	70	99	99	99	99	97	82
South American Butterflies	60	70	77	84	84	89	91	91	91	81	82
European Marine Fish	80	72	72	85	86	83	84	80	78	69	79
North American Birds	61	67	73	74	76	81	83	83	84	87	77
Amazonian Moths	72	43	42	88	75	87	90	90	91	89	77
North European Tachinidae	71	60	66	77	80	77	84	82	82	84	76
French Guianan Earthworms	78	89	93	81	81	73	80	70	59	55	76
Northwest Pacific Molluscs	76	75	75	77	77	76	77	76	76	63	75
German Aranea & Opiliones	76	18	79	85	82	71	74	73	65	52	67
Congolese Fish	68	44	55	67	71	70	63	67	71	65	64
Tanytarsus	67	71	71	61	62	50	56	48	47	45	58
North American Pyraustinae	25	29	41	67	76	70	74	67	58	59	57
Ecuadorian Chrysomelidae	55	55	54	56	56	57	57	55	57	58	56
Iberian Butterflies	26	36	42	53	57	60	65	59	55	52	50
Consolidated:	**69**	**63**	**71**	**80**	**79**	**80**	**82**	**81**	**79**	**74**	**76**
6 Clade-based Datasets											
Coleoptera	77	80	80	81	82	77	79	76	73	67	77
Diptera	69	73	74	76	77	73	75	72	69	63	72
Lepidoptera	42	54	62	74	77	79	78	79	77	71	69
Arachnida	71	71	71	69	68	66	64	64	64	57	67
Actinopterygii	59	54	55	64	64	66	66	65	65	64	62
Hymenoptera	62	64	65	64	65	62	63	62	59	55	62
Consolidated:	**63**	**66**	**68**	**72**	**73**	**71**	**72**	**71**	**69**	**64**	**69**
Overall Consolidated:	**65**	**65**	**68**	**74**	**74**	**73**	**74**	**73**	**71**	**66**	**70**

PTP

Length	94	130	145	164	189	295	307	313	407	657	Average
Midpoint	**257**	**65**	**73**	**243**	**213**	**405**	**154**	**502**	**455**	**329**	
20 Empirical Datasets											
Great Barrier Reef Fish	89	85	87	91	91	95	90	95	96	96	91
Pakistani Lepidoptera	95	83	82	87	90	95	95	95	95	94	91
Ecuadorian Geometridae	14	89	91	94	97	98	97	96	99	98	87
North Sea Molluscs	78	71	82	94	96	86	92	86	93	93	87
South China Sea Fish	86	75	77	87	88	92	89	89	92	92	87
Canadian Echinoderms	75	71	78	83	90	89	90	87	91	89	84
German EPT	82	80	81	81	83	79	83	82	79	80	81
North European Tachinidae	77	70	73	82	80	84	83	83	82	85	80
Amazonian Moths	32	88	38	89	88	91	89	91	90	90	79
German Aranea & Opiliones	72	73	77	77	79	82	80	77	81	79	78
North American Birds	72	67	66	77	78	81	82	81	85	85	77
French Guianan Earthworms	71	83	69	85	80	81	62	78	75	69	75
European Marine Fish	71	60	61	71	78	80	74	79	79	80	73
Northwest Pacific Molluscs	72	67	68	75	74	72	74	76	77	78	73
Congolese Fish	57	44	50	67	69	68	64	68	71	69	63
Tanytarsus	51	58	64	61	58	68	63	64	66	63	62
North American Pyraustinae	45	58	54	56	49	58	71	80	76	58	61
Ecuadorian Chrysomelidae	55	57	55	56	55	55	54	55	55	55	55
Iberian Butterflies	32	47	48	47	48	59	58	61	58	54	51
South American Butterflies	0	0	0	0	0	89	90	93	91	91	45
Consolidated:	**63**	**68**	**66**	**74**	**75**	**81**	**81**	**82**	**82**	**82**	**76**
6 Clade-based Datasets											
Coleoptera	74	73	73	78	78	81	81	80	81	80	78
Arachnida	69	70	70	70	69	70	68	68	68	66	69
Diptera	37	71	69	55	71	76	76	75	75	75	68
Lepidoptera	39	65	41	64	33	79	78	77	79	78	63
Hymenoptera	44	63	63	62	64	66	66	65	65	65	62
Actinopterygii	22	49	51	61	61	64	61	64	65	65	56
Consolidated:	**45**	**64**	**59**	**65**	**61**	**73**	**72**	**72**	**73**	**72**	**66**
Overall Consolidated:	**50**	**65**	**61**	**67**	**64**	**75**	**74**	**74**	**75**	**74**	**68**

Figure 3. Match ratios across three different species delimitation methods. Mini-barcodes (columns) are sorted by primer length while the 20 empirical datasets (rows) are sorted by average match ratio. The six clade-specific datasets from GenBank are grouped below. Match ratios above average are coloured green, while those below average are in pink. The highest match ratio values are indicated with white text.

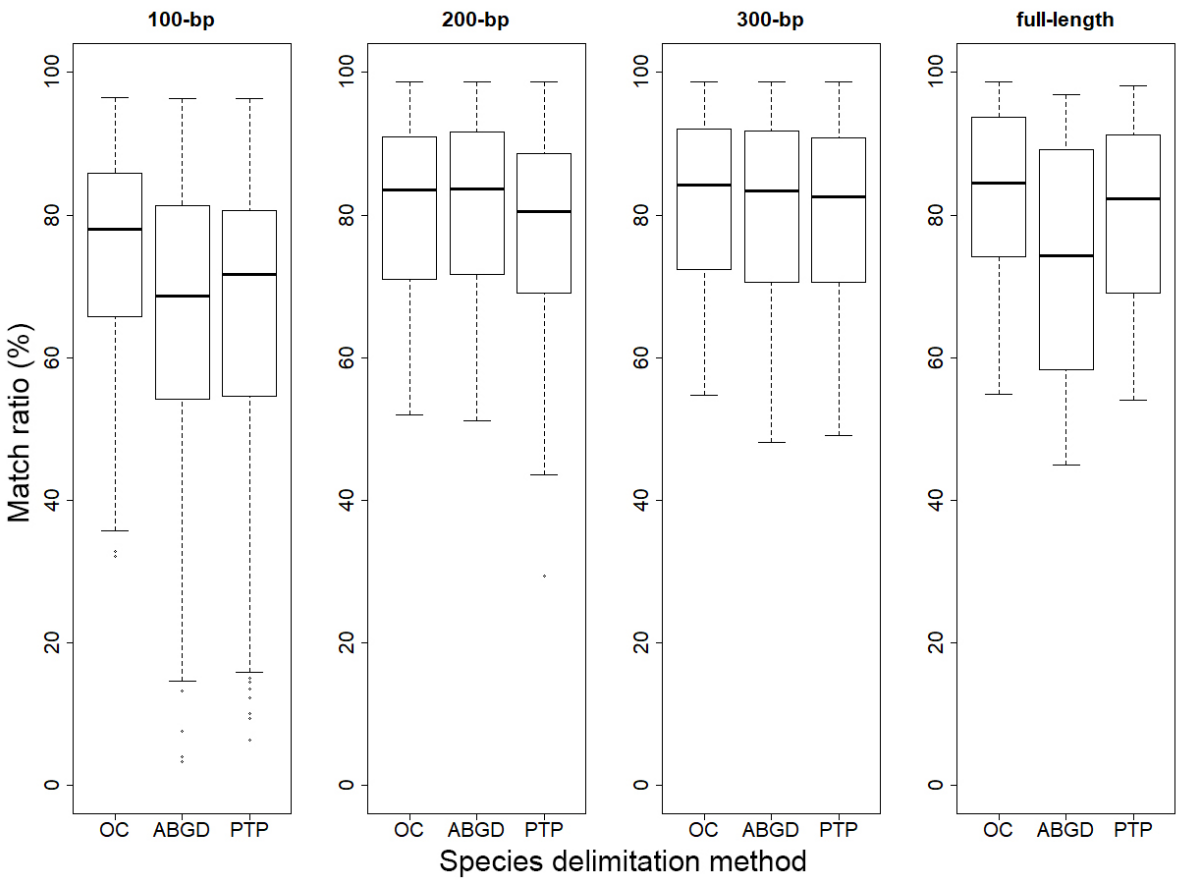

1068

1069 **Figure 4.** Comparison of species delimitation methods for full-length and mini-

1070 barcodes generated by “sliding windows” (100-bp, 200-bp, 300-bp).

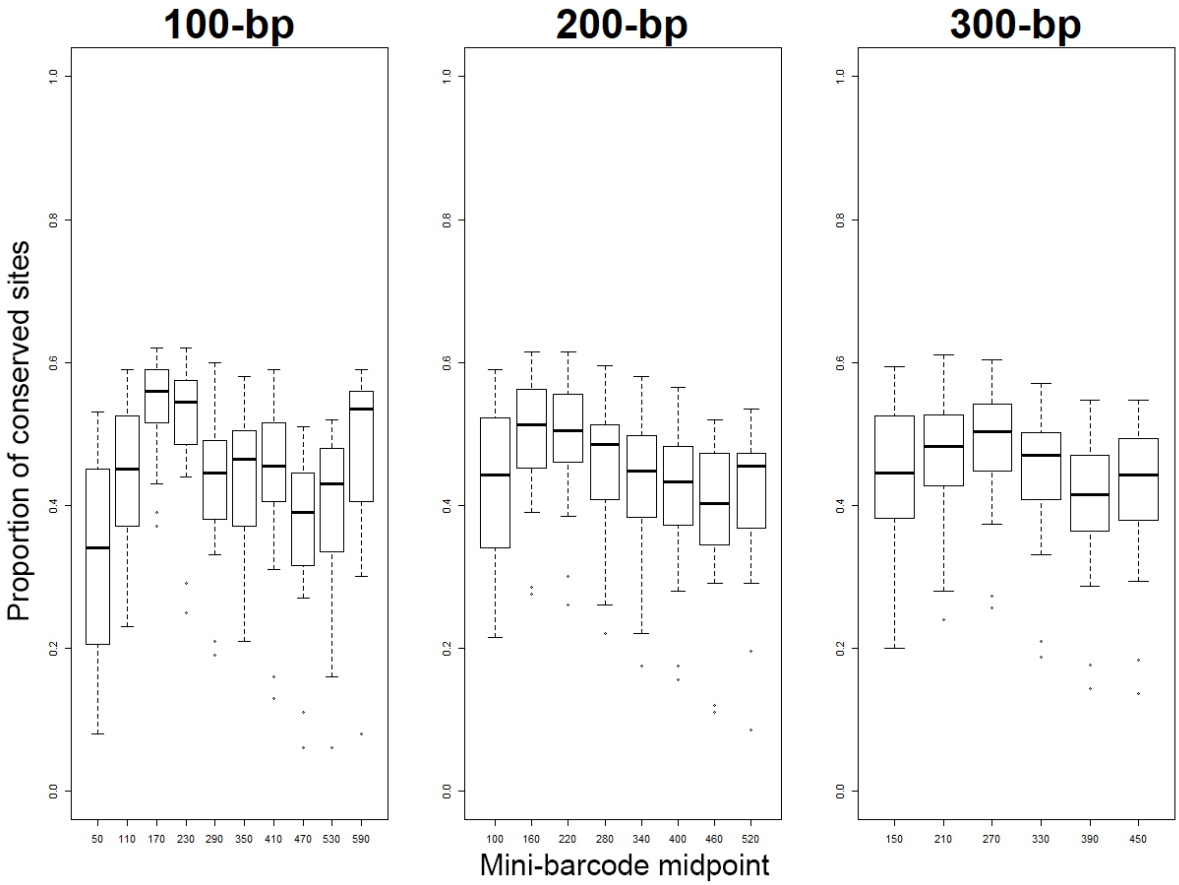

Figure 5. Proportion of conserved sites along the full-length barcode (sliding windows of 100-bp, 200-bp, 300-bp).